

The structures of phenolic oximes and their complexes

Andrew G. Smith, Peter A. Tasker*, David J. White

Department of Chemistry, University of Edinburgh, West Mains Road, Edinburgh EH9 3JJ, UK

Received 11 January 2001; accepted 21 November 2002

Contents

Abstract	61
1. Introduction	62
1.1 Background	62
1.2 Nomenclature	63
1.3 Data sources	63
2. Phenolic oxime ligands	63
2.1 Simple phenolic oxime ligands	63
2.2 Phenolic oxime ligand hydrogen bond adducts	66
3. Phenolic oxime complexes	67
3.1 First row transition metals	67
3.1.1 Vanadium	67
3.1.2 Chromium	70
3.1.3 Manganese	70
3.1.4 Iron	70
3.1.5 Cobalt	72
3.1.6 Nickel	73
3.1.7 Copper	74
3.1.8 Zinc	76
3.1.9 Mixed first row transition metal complexes	76
3.2 Second and third row transition metals	77
3.2.1 Molybdenum	77
3.2.2 Palladium	78
3.2.3 Platinum	78
3.3 Complexes of other element	78s
3.3.1 Boron	78
3.3.2 Gallium	79
3.3.3 Tin	80
4. Table's of phenolic oxime ligands and metal complexes	81
5. Summary and conclusions	81
Acknowledgements	84
References	84

Abstract

This review article describes the rich coordination chemistry of phenolic oxime ligands based on solid state structures in the October 2000 release of the Cambridge Structural Database. The phenolic oxime ligands discussed have the general formula $n-(R_1)_x-2-OH-C_6H_{4-x}C(R_2)NOH$. Whilst their classical mode of coordination via the deprotonation of the phenol to bind to a the metal centre as a mono-anionic bidentate ligand is frequently observed, the structural survey reveals a plethora of less common binding motifs that can be attained via the deprotonation of both the phenolic and oximic hydrogens resulting in the formation of tridentate ligands and polynuclear bridged complexes. The formation of such polynuclear complexes at surface sites may account for

* Corresponding author.

E-mail address: p.a.tasker@ed.ac.uk (P.A. Tasker).

their efficacy as corrosion inhibitors. Also highlighted is the occurrence of hydrogen bonding between oximic hydrogen and phenolic oxygen atoms and its implications on the thermodynamic stability of metal complexes via the formation of pseudo-macrocylic motifs and on the pre-organisation of dimeric metal-free ligand species. The formation of ligand–ligand hydrogen bonds to define donor cavities of a well defined size accounts for their remarkable selectivity when used in commercial metal recovery processes based on solvent extraction.

© 2002 Elsevier Science B.V. All rights reserved.

Keywords: Salicylaldoximes; 2-Ketophenoloximes; Metal-oxime complexes; Bridging oximate ligands; Metal-extractants

1. Introduction

1.1. Background

Phenolic oximes with the generic structure shown in Fig. 1 find extensive use in industry, mainly as extractants for copper, [1] but also as anticorrosives in protective coatings [2].

Their role in copper recovery is to effect both the ‘concentration’ and ‘separation’ unit operations of metallurgy [3] by solvent extraction. These types of extractant are currently used in solvent extraction plants world-wide, producing over 2.3 million tonnes of copper per annum, around one fifth of the total world production [1,4]. A typical flowsheet is outlined in Fig. 2.

In order to fulfil this role the ligand must show a remarkable selectivity for complex formation of cop-

per(II) over other metals in the pregnant leach solution, notably over ferric iron which is usually present at comparable or higher concentrations. Complex formation must be favourable at the relatively low pH values (<2.0) required to ensure that ferric iron remains in solution. Such ‘strength’ and selectivity of complex formation with copper have been assumed [5,6] to arise from a very favourable goodness-of-fit for the bonding

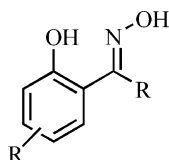


Fig. 1. Generic phenolic oxime structure.

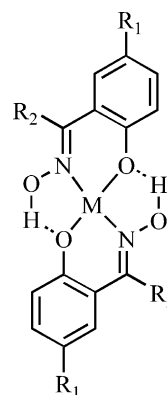


Fig. 3. Hydrogen bonding between phenolic oxime units in 2:1 complexes.

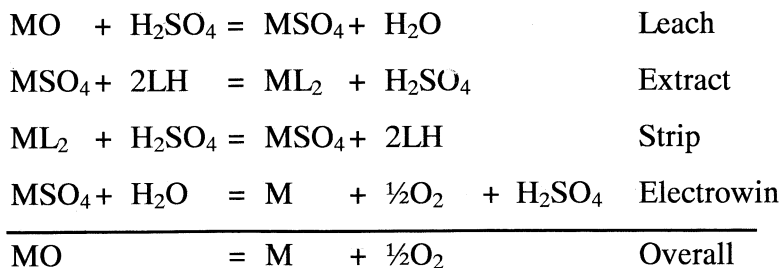
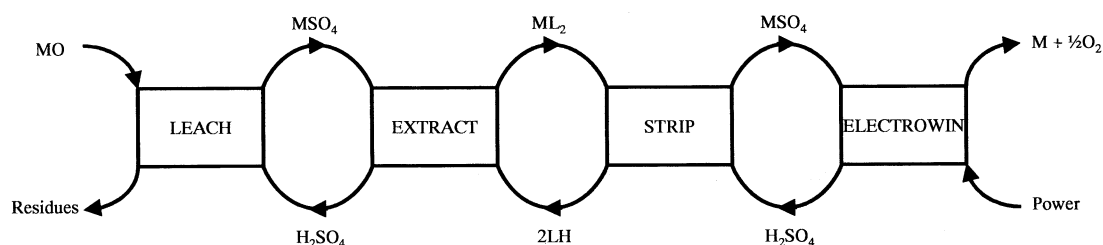


Fig. 2. Flow sheet and mass balance for copper production using a phenolic oxime extractant.

cavity in the ligands which is defined by hydrogen bonding between two bidentate units (Fig. 3). The extent to which such intramolecular hydrogen bonding in complexes leads to special stability by generating pseudo-macrocyclic systems is thus a structural feature of considerable practical significance in determining the efficiency of these extraction processes.

Another feature of the phenolic oxime ligands is their propensity [7,8] to form polynuclear complexes in which both the oxime and phenolate functions can act as bridging units. Formation of such complexes at lightly oxidised iron surfaces may [2] be an important factor in the mode-of-action of phenolic oximes in protective coatings leading to high kinetic and thermodynamic stability of the oxide | polymer interfaces.

In this review we will focus on the structures of phenolic oxime complexes and examine how the formation of ‘simple’ mononuclear complexes involved in solvent extraction, or of polynuclear complexes of the types proposed for metal surface protection, depend on the nature of the metal and on aspects of ligand design. Hydrogen bonding between ligands is an important structural feature. The extent to which this could influence preorganisation of donor sets will be addressed by considering the solid state structures of metal-free forms of the ligands.

The commercial importance of these reagents has fuelled extensive research into the basic chemistry of phenolic oxime ligands. It is hoped that this review of their solid state chemistry will give insight into the common structural features and peculiarities of their metal complexes. In particular, the versatility of the ligands will be exemplified. Further, it is hoped that this might be used as a predictive tool to elucidate the coordination chemistry of these ligands with other, as yet unexplored, Lewis acids.

1.2. Nomenclature

The general form of phenolic oxime ligand to be discussed in this review is given in Fig. 4. Historically, these have been referred to as ‘salicylaldoxime type’ ligands and the shorthand nomenclature used here is based on the abbreviation *sal* to denote the general form of the ligand. The 2-hydroxy-benzaldehyde oxime central core can be modified by replacing the aldehydic hydrogen with a substituent or by placing substituents

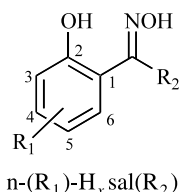


Fig. 4. The general form of and abbreviations used for ligands in this review.

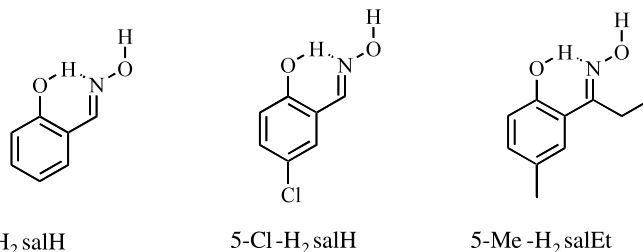


Fig. 5. Examples of phenolic oxime ligands with abbreviations.

on the aromatic ring. When forming metal complexes the phenolic proton is almost invariably replaced, but it is also possible for the less acidic proton to be lost from the oximic oxygen atom. The abbreviations used here have been chosen to provide a concise description of the substitution pattern and to denote the protonation level of the ligand (see Fig. 4).

The aromatic substituents are denoted first with their substitution positions, followed by an indication of the level of ligand protonation, ‘H₂’ for free ligand, ‘H’ for the monoanion and nothing for the dianion. Finally the substitution at the oximic carbon atom is given. Examples are provided in Fig. 5.

1.3. Data sources

The structures discussed here appear in Version 5.20 (October 2000 release) of the CCDC database [9]. They were identified by searching for the fragment shown in Fig. 6 and the 167 hits were sorted manually to eliminate non phenolic oxime structures. The remaining 58 structures, some of which are duplicates, are listed in Tables 7 and 8 for ligands and complexes, respectively.

The remaining structures were taken from Ph.D. theses produced either at the University of Manchester or the University of North London. Full details are given in the references [10–13].

2. Phenolic oxime ligands

2.1. Simple phenolic oxime ligands

Of the 12 uncomplexed phenolic oximes in the Cambridge Crystallographic Database, 2-hydroxy benzaldehyde oxime, H₂salH, in the orthorhombic form, appears to be incorrect [14] and has been redetermined [15] and

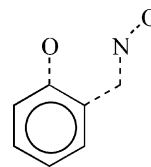


Fig. 6. General search fragment used to interrogate the CCDC database. Dotted lines represent ‘any’ bond. The ring system was defined as aromatic.

5-Et-H₂salMe, has been duplicated [16,17]. Four have no structural or coordinate data [16] leaving six published structures available for analysis. Four more previously unpublished structures [11,13] are included here (see Table 7).

Hydrogen bonding is a major feature of these structures. This results from the high density of hydrogen bonding donors and acceptors per molecule. Invariably the phenolic proton forms an intramolecular hydrogen bond to the nitrogen of the oxime group giving a six membered ring (Fig. 7). Since the phenolic proton has not been found from Fourier difference

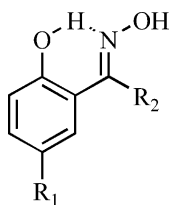


Fig. 7. Intramolecular hydrogen bond forming a six membered ring that is seen in all phenolic oximes. R = H, alkyl, aryl.

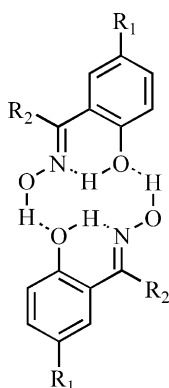


Fig. 8. The pseudo-macrocyclic assembly seen in aldoximes when R₁ and R₂ are monatomic substituent.

maps in the majority of the structures, we will characterise this interaction in terms of the phenolic oxygen to oximic nitrogen separation. This distance varies little between structures with a maximum value of 2.65 Å and a minimum of 2.51 Å. However, a general trend is that aldoximes have a greater phenolic O...N distance (mean 2.63 Å) than the ketoximes (mean 2.52 Å).

In all of the free ligand structures the molecules associate via intermolecular hydrogen bonding. With the exception of the adducts formed with diamines (see section 2.2.2), these structures fall into two categories. Dimers result from the interaction of the oximic proton with an adjacent phenolic oxygen to produce a pseudo-macrocyclic ligand with a 14 membered inner great ring (shown schematically in Fig. 8). This structure is only seen for aldoximes with no substituents or only monatomic substituents on the aromatic ring, i.e. for H₂salH [15] and 5-Cl-H₂salH [18]. The O...O distances involved in the hydrogen bonded interaction in both of these centrosymmetric dimers are very similar (2.82 and 2.83 Å). Fig. 9 shows two views of the solid state structure of 5-Cl-H₂salH. The top view clearly shows the pseudo-macrocyclic dimeric structure. Although the phenolic oxime is almost planar, the dimeric units are not. The molecular planes run parallel but are separated by a distance δ (side view in Fig. 9). The value of δ is 0.30 Å for H₂salH and 1.4 Å for 5-Cl-H₂salH. This 'step' configuration is also seen, but to a lesser extent, in the metal complexes (vide infra). The step configuration in the free ligand dimers increases the separation between the phenolic protons over that expected in a planar form, e.g. in [5-Cl-H₂salH]₂ this distance is 2.98 Å compared with 2.74 Å calculated for a flattened configuration with the same intermolecular hydrogen bonding distance. The step configuration provides a compromise in allowing two favourable intermolecular hydrogen bonds in the dimer whilst minimising the

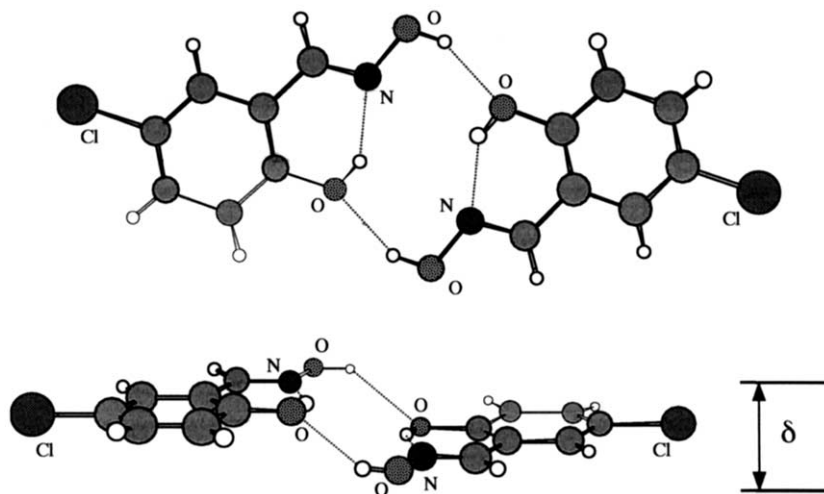


Fig. 9. Top and side views of the dimeric solid state structure of 5-Cl-H₂salH.

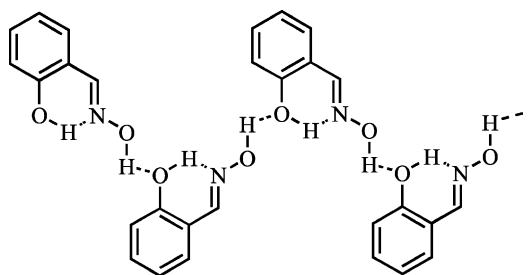


Fig. 10. Schematic of the hydrogen bonding seen in the polymeric form of the free ligands.

repulsion between the two phenolic protons. The geometry of the N_2O_2 donor set provided by the oxime nitrogen atoms and the phenol oxygen atoms in these dimers is similar to that in planar ML_2 pseudo-macrocyclic metal complexes (such as those seen for copper discussed in Section 3.1.7) and infers that the ‘strength’ and selectivity of complexation will be favourable for such metals (see Section 3.1.7).

The introduction of groups which remove planarity in the molecule appears to stop efficient packing of dimeric units in the crystal and, instead, a polymeric structure $[(H_2sal)_n]$ is observed (shown schematically in Fig. 10). This is true for all phenolic ketoximes and for phenolic aldoximes which have bulky substituents on the aryl ring. An example is given in Fig. 11 that shows the solid state structure of 5-MeO- H_2salH [19]. The linear polymeric array of hydrogen bonds also provides two hydrogen bonds per phenolic oxime unit but in this arrangement the intermolecular bond is stronger, as judged by the range of $O \cdots O$ distances, (2.73–2.82 Å) than that in the dimers. In the polymeric arrangement a closer approach of the oxygen atoms is not compromised by repulsive interactions between the phenolic protons, as in the dimers.

It is of interest to speculate as to why these two structural modifications are observed. There are several possibilities:

- 1) There may be a fine balance between hydrogen bonds and crystal packing forces that determines which of the modifications is observed. More planar molecules, which can form the layer type structure, dimerize. Non planar molecules with bulky substituents, which are unable to pack efficiently in this layer type structure, form polymeric chains.
- 2) The solvent of crystallisation may play an important role. It has been shown by vapour pressure osmometry and cryoscopy [20,21] that the association number in solution (a measure of oligomerisation) is highly solvent dependent, approximating to one in polar protic and aromatic solvents (monomer) but greater than one in aliphatic hydrocarbon solvents (dimer or oligomer). The predominant solution species may determine the modification that crystallises. Unfortunately, in several of the systems discussed here, the recrystallisation solvent is not reported. If solvent is important, it may be possible to crystallise different polymorphs from different solvents, although there are examples of both polymers and dimers recrystallised from alcohol.
- 3) Just as solvent is important in determining solution association number, so is concentration. The same arguments as above will apply. The concentration of the solution from which crystals are obtained is not commonly reported and is not given in any of the systems discussed. Local concentration within solution and, therefore, the method of crystallisation, saturation, evaporation or precipitation, may also be important.

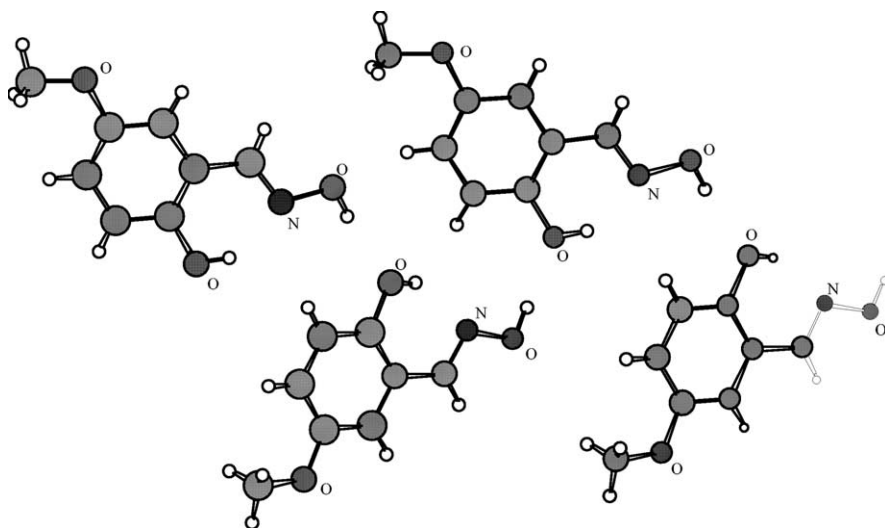


Fig. 11. Polymeric form of hydrogen bonding seen in ketoximes and ‘non planar’ substituted aldoximes. The compound shown is 5-MeO- H_2salH .

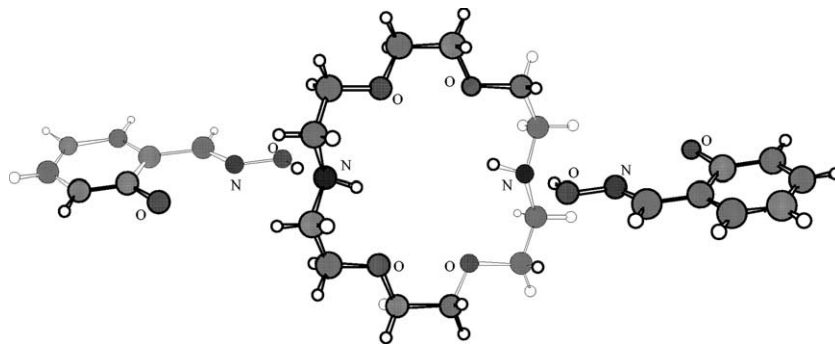


Fig. 12. Structure of 2:1 adduct of H_2salH with diaza-[18]-crown-6.

With the limited data set it is impossible to be conclusive, but the first of these possibilities may be the most convincing. As more structures become available it may be possible to gain a better understanding of the factors that control the crystallisations.

2.2. Phenolic oxime ligand hydrogen bond adducts

The high density of hydrogen bond donors and acceptors in phenolic oxime ligands means that they will co-crystallise with other hydrogen bond donor and acceptor molecules. One example of this appears in the literature, and a further unpublished example will be discussed here.

Watson, Vogtle et al. [22] have shown that heating a solution of H_2salH with the macrocycle diaza-[18]-crown-6 in ethylacetate, followed by slow cooling gives poor quality crystals which were characterised by X-ray crystallography as the 2:1 oxime:crown adduct (Fig. 12). Although not located in difference Fourier maps, the phenolic proton is assumed to form an intramolecular hydrogen bond to the oxime nitrogen, as in all the free ligand structures. The oximic protons were located in hydrogen bonds with nitrogen atoms of the diaza crown ($O \cdots N$ 2.682(9) Å) which 'pin down' the amine nitrogen atoms of the macrocycle, showing much lower anisotropic displacement parameters than the rest of the molecule. The observed density of the crystal is very low and suggests that the structure is inefficiently packed.

A second example of a phenolic oxime–amine adduct is provided by the unpublished structure of the 2:1 adduct of H_2salH with tetramethyl ethylenediamine [$(H_2salH)_2(tmeda)$]. The combination of two intra and two intermolecular hydrogen bonds in the centrosymmetric adduct (Fig. 13) is similar to that seen with diaza-18-crown-6, but with much more efficient packing in the solid state [13].

The NCCN backbone of the tmeda molecule is almost planar ($N-C-C-N$ torsion angle 179.97°) and the nitrogen atoms are antiperiplanar (shown as a Newman projection in Fig. 14).

It is somewhat surprising that these adducts can be isolated since, on the basis of the strength of $OH \cdots O$ versus $OH \cdots N$ hydrogen bonds, we might expect the simple hydroxy oxime ligand to be the predominant species in all cases. However, solution NMR studies

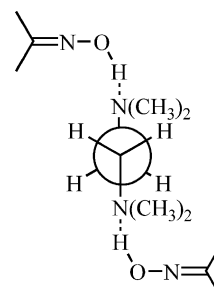


Fig. 14. Newman projection showing conformation of [$(H_2salH)_2(tmeda)$].

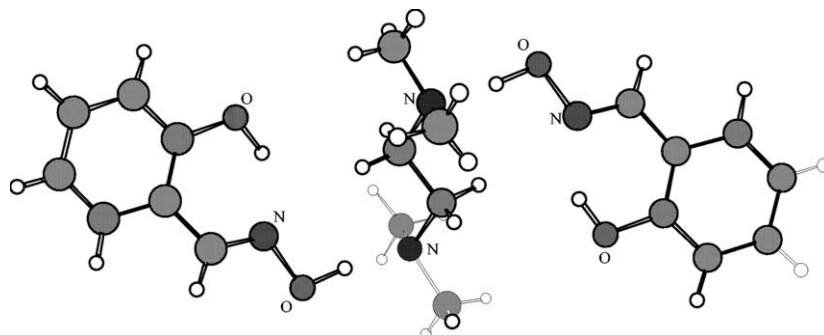



Fig. 13. Solid state structure of [$(H_2salH)_2(tmeda)$].

H																	He
Li	Be											B	C	N	O	F	Ne
Na	Mg											Al	Si	P	S	Cl	Ar
K	Ca	Sc	Ti	V	Cr	Mn	Fe	Co	Ni	Cu	Zn	Ga	Ge	As	Se	Br	Kr
Rb	Sr	Y	Zr	Nb	Mo	Tc	Ru	Rh	Pd	Ag	Cd	In	Sn	Sb	Te	I	Xe
Cs	La	La	Hf	Ta	W	Re	Os	Ir	Pt	Au	Hg	Tl	Pb	Bi	Po	At	Rn
Fr	Ra	Ac															
			Ce	Pr	Nd	Pm	Sm	Eu	Gd	Tb	Dy	Ho	Er	Tm	Yb	Lu	
			Th	Pa	U	Np	Pu	Am	Cm	Bk	Cf	Es	Fm	Md	No	Lr	

 Phenolic oxime complex known

have shown that this is not what is observed and amine oxime adducts readily form.

3. Phenolic oxime complexes

The Cambridge Database contains complexes of phenolic ligands with the elements shown in Fig. 15 and Table 8. The first row transition metals, second and third row transition metals, p block and mixed metal systems will be discussed in the following sections.

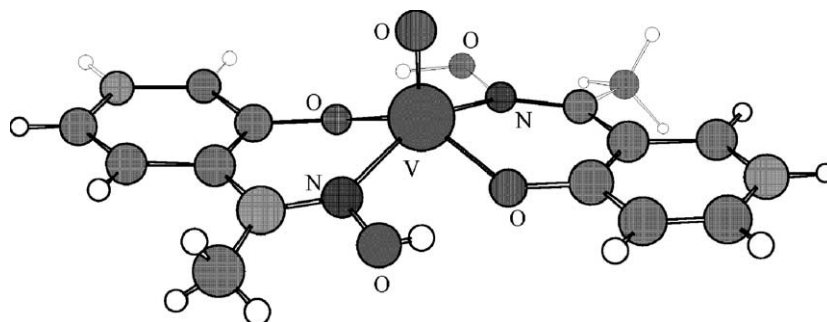
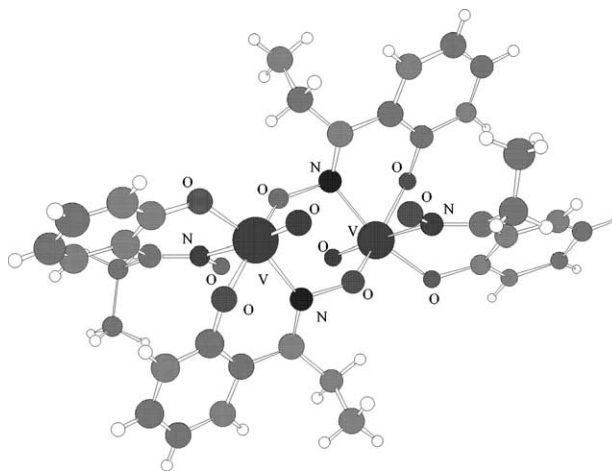
3.1. First row transition metals

3.1.1. Vanadium

Reaction of vanadyl sulfate with phenolic oximes leads to the formation of neutral vanadium(IV) $[\text{VO}(\text{HsalR})_2]$ complexes. The complex $[\text{VO}(\text{HsalMe})_2]$ has the pseudo-macrocyclic structure with a hydrogen bond stabilised *trans* arrangement of the ligands (Fig. 16) [12]. The step structure in the complex (vide supra) is not observed and the aryl and chelate rings form a plane. The vanadium atom lies 0.6 Å above this plane and the V=O bond is inclined to it at an angle of 87°.

Although many of the applications of salicylaldoximes rely on the high stability of their metal complexes, vanadyl bis phenolic oxime complexes show instability in a range of organic solvents [24–26]. On dissolution in hydrocarbon or chlorinated solvents the original lilac solutions of these phenolic oxime complexes deepen to violet and precipitation occurs. Structural studies of the

reaction products of [VO(HsalH)₂], [VO(HsalMe)₂] and [VO(HsalEt)₂] show that oxidation has occurred to give dimeric vanadium(V) complexes of the general formula [{VO(HsalR)(salR)}₂] [11,12]. The vanadium(IV) salicylaldoxime complex [VO(HsalH)₂] deposits black crystals from chloroform solution which contain the dimer [{VO(HsalH)(salH)}₂] with a V...V separation of 4.0 Å. Each vanadium is 6-coordinate and has distorted octahedral geometry. The vanadium ions are coordinated by a vanadyl oxygen, a phenolic oxygen and a nitrogen from one monodeprotonated oxime ligand, and a phenolic oxygen and a nitrogen from a doubly deprotonated ligand. The final coordination site is occupied by an oxime oxygen from a ligand on the



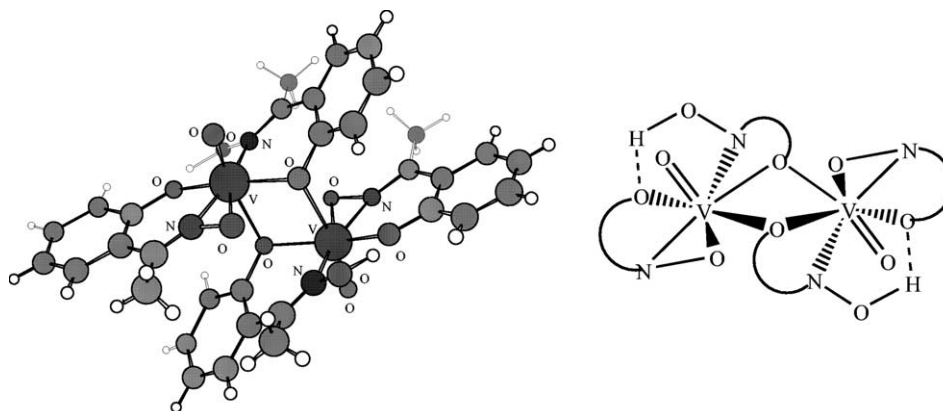


Fig. 18. The solid state structure and a schematic representation of $[\{VO(HsalMe)(salMe)\}_2]$.

adjacent vanadium and hence dimer formation is achieved. A very similar structure (Fig. 17) is shown by the dimer $[\{VO(HsalEt)(salEt)\}_2]$, which is also deposited from chloroform, but with a slightly shorter $V \cdots V$ distance of 3.94 Å.

The structure of the product of oxidation of $[VO(HsalMe)_2]$ in 1,2-dichloroethane, $[\{VO(HsalMe)(salMe)\}_2]$, although dimeric, has a remarkably different structure [12]. In this case the $V \cdots V$ distance is markedly shorter at 3.45 Å and the vanadium atoms are heptacoordinate with pseudo-pentagonal bipyramidal geometry (Fig. 18). Three of the equatorial sites are occupied by a phenolate oxygen and both the nitrogen and oxygen atoms of one oxime in an η^2 binding mode. The oxime nitrogen and phenolate oxygen of a second mono-deprotonated ligand define the remaining two equatorial sites in a conventional chelating mode. This phenolate oxygen atom provides a bridge to the second

vanadium atom in an apical site. The other apical site is occupied by the vanadyl oxygen atom. Thus the mono-deprotonated $[HsalMe]^-$ acts as a bridge, whilst the doubly deprotonated ligand $[salMe]^{2-}$ shows an unprecedented tridentate binding mode using the phenolate oxygen atom and both the N and O atoms of the oximate group. Intramolecular hydrogen bonds between the NOH groups and the non-bridging phenolates further stabilise the structure which is shown schematically in Fig. 18.

The products obtained on dissolution of $[VO(HsalR)_2]$ in organic nitriles have been determined [27]. Structure determination (Fig. 19) of the product of reaction of vanadyl-bis-salicylaldoximate with acetonitrile shows that the oxime OH group adds across the $C \equiv N$ of the nitrile yielding a new tridentate N_2O^- ligand. This ligand coordinates to the oxidised *cis* dioxo vanadium(V) centre giving a distorted square-based pyramidal geometry.

Reaction of H_2salH with $[VO(acac)_2]$ in methanol gives only low yields of $[VO(HsalH)_2]$, as a green powder, but on standing a second red-brown product $[V_3O_3(OMe)_5(salH)_2]$ is obtained. The ethoxo derivative $[V_3O_3(OEt)_5(salH)_2]$ has been similarly obtained in ethanol and has been structurally characterised [28]. This trinuclear complex has *ca.* C_2 symmetry. Each $(salH)^{2-}$ ligand chelates one vanadium atom through the phenolate oxygen and oxime nitrogen, while bridging to the remaining two vanadiums through the deprotonated oxime oxygen. Each vanadium has a terminal oxo group and there are two bridging and three terminal ethoxides (Fig. 20).

If the reaction is instead carried out under reflux, a third, red-brown product is obtained. X-ray crystallography shows this to be $[VO(OMe)(OC_6H_4CH=NCHC_6H_4OC(O)(Me)CHCOMe)]$ (see Fig. 21). The template formation of this novel tetradentate ligand apparently involves the coupling of one mole of acetylacetone, one mole of salicylaldehyde (presumably in turn a reaction

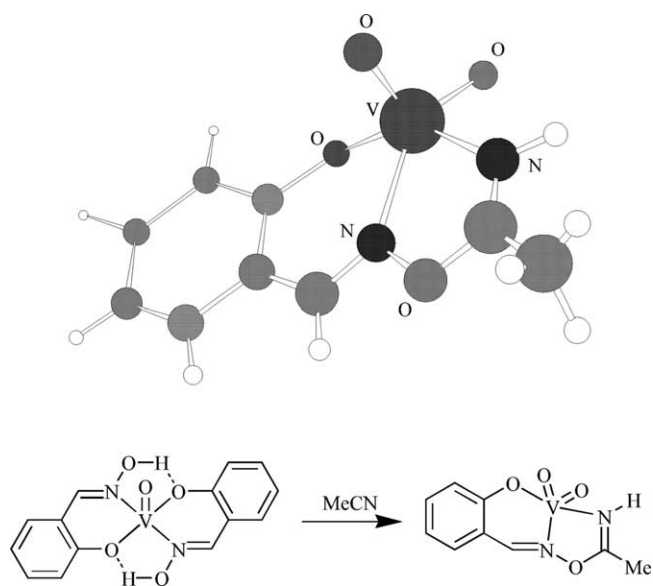
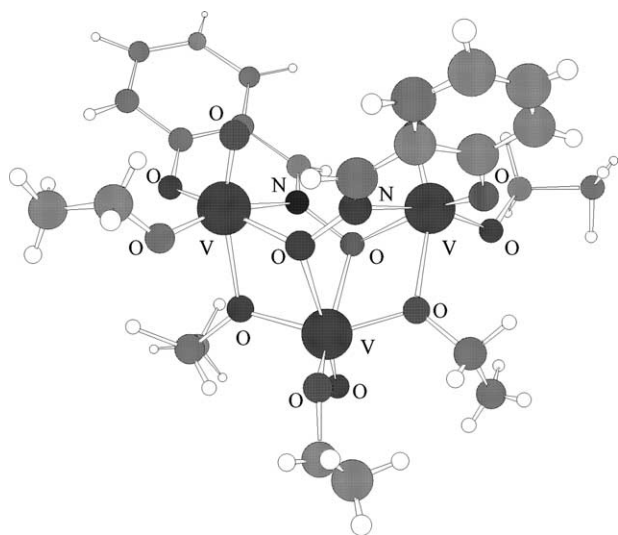
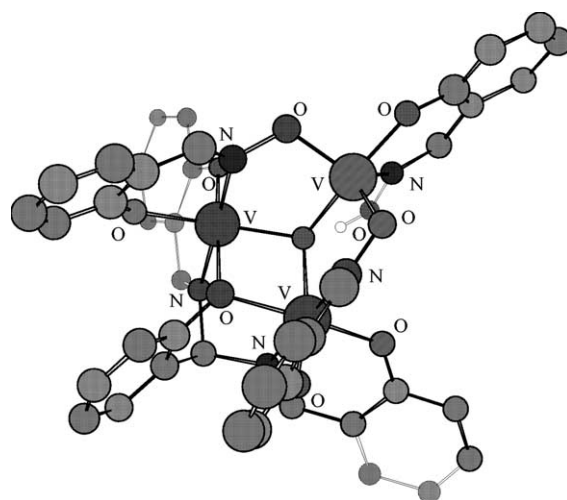


Fig. 19. Reaction of vanadyl-bis-salicylaldoximate with acetonitrile and the solid state structure of the product, $[V(V)O_2\{C_6H_4(O)CH=N-OC(Me)=NH\}]$.

Fig. 20. Solid state structure of $[V_3O_3(OEt)_5(salH)_2]$.

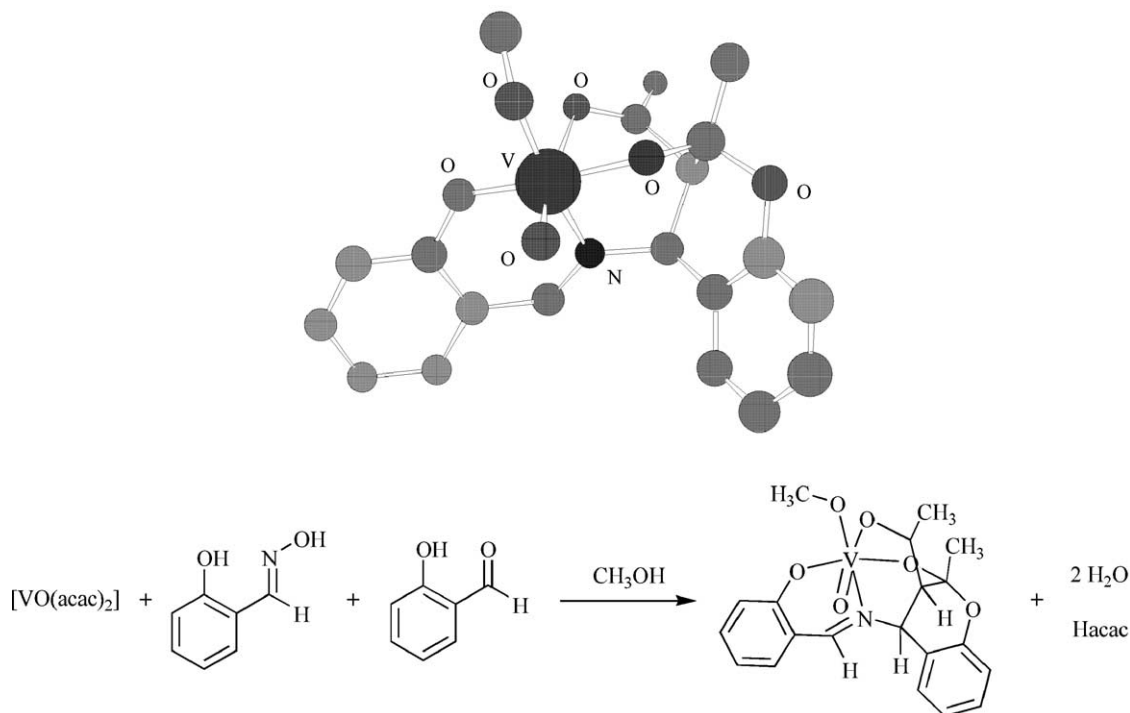
product of salicylaldehyde), with loss of two moles of water.

Vanadium(II) bromide with H_2salH and triethylamine in dry methanol under argon gives a dark green solution from which green crystals of $[Et_3NH][V_3(\mu_3-O)(HsalH)(salH)_2(salmp)] \cdot 2H_2O$ which is isostructural with the iron(III) analogue discussed later in Section 3.1.4 (see Fig. 27) [29]. The asymmetric triangular vanadium(III) complex contains the novel $[V_3(\mu_3-O)(\mu_2-OR)]^{6+}$ core unit, Fig. 22. This trinuclear motif appears in the related Ti(III), Cr(III), Mn(III), Fe(III)

Fig. 22. Solid state structure of $[V_3(\mu_3-O)(HsalH)(salH)_2(salmp)]^-$ excluding the hydrogens for clarity.

and Co(III) complexes prepared in a similar manner, and is discussed further for the related Fe(III) complex in Section 3.1.4.

The three vanadium ions lie at the apices of an isosceles triangle with the μ_3 -oxide atom displaced from the plane by 0.52 Å. Its disposition is not symmetrical within the triangle with one of the V–O bonds being 0.04 Å shorter than the other two, which are statistically similar (V–O, 1.97 Å). Two of the vanadium atoms are in a distorted octahedral environment with N_2O_4 coordination spheres and the third is 5-coordinate

Fig. 21. Solid state structure of $[VO(OMe)(OC_6H_4CH=NCHC_6H_4OC(O)(Me)CHCOMe)]$ produced from the coupling reaction of acetylacetone, salicylaldehyde and salicylaldehyde with $[VO(acac)_2]$. The hydrogen atoms have been excluded for clarity.

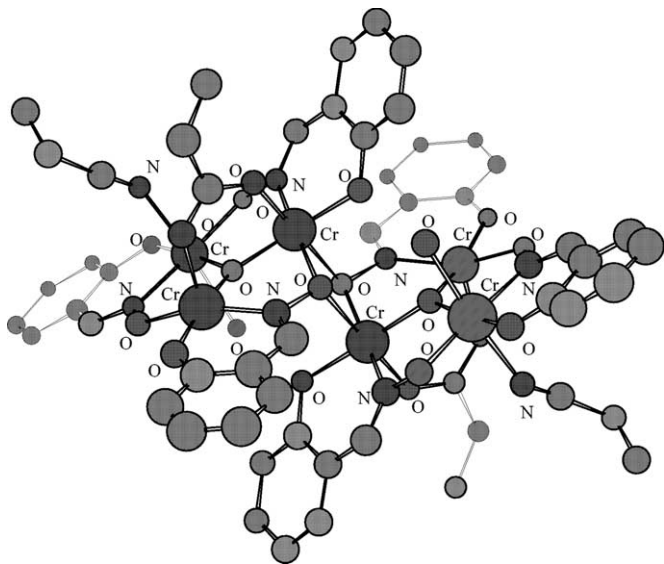


Fig. 23. Structure of $[\text{Cr}_6(\mu_3\text{-O})_2(\text{salH})_6(\mu_2\text{-OOCC}_2\text{H}_5)_2(\text{OH}_2)_2(\text{C}_2\text{H}_5\text{CN})_2]$, excluding hydrogen atoms for clarity.

trigonal bipyramidal with an NO_4 donor set. The complex is further stabilised by a hydrogen bond between the oximic hydrogen on the mono deprotonated salicylaldoxime and the $\mu_3\text{-O}$ atom ($\text{O}\cdots\text{O}$, 2.677(6) Å).

3.1.2. Chromium

One chromium containing complex of a phenolic oxime has been structurally reported in the literature [30]. The only other example of a chromium containing phenolic oxime complex, with a reported X-ray structure, is a mixed iron/chromium system (see Section 3.1.9).

The addition of H_2salH and triethylamine to a previously prepared green solution of CrF_2 and CaCl_2 in methanol and propanoic acid affords a brown solution. Recrystallisation from propionitrile produces brown crystals of $[\text{Cr}_6(\mu_3\text{-O})_2(\text{salH})_6(\mu_2\text{-OOCC}_2\text{H}_5)_2(\text{OH}_2)_2(\text{C}_2\text{H}_5\text{CN})_2]$, shown in Fig. 23. The hexanuclear structure comprises of two identical $\mu_3\text{-oxo}$ centred trinuclear $[\text{Cr}_3(\mu_3\text{-O})]$ units. The chromium ions form an isosceles triangle ($\text{Cr}\cdots\text{Cr}$, 3.148(1), 3.263(1), 3.252(1) Å) with the $\mu_3\text{-O}$ atom placed almost centrally within the triangle with an average $\text{Cr}\text{--}\text{O}$ length of 1.87 Å. The two units are related by inversion symmetry and linked via two μ_2 -bridging oxygen oxime atoms with a slightly longer $\text{Cr}\cdots\text{Cr}$ separation of 3.275(2) Å. Two of the three chromium atoms in each triangle unit have distorted octahedral environments with coordination spheres of N_2O_4 and NO_5 . The remaining chromium is 5-coordinate, providing a rare example of a non-octahedral Cr(III) , and is best described as square-pyramidal with a NO_4 donor set. A similar M_6O_2 core is found in complexes with other trivalent metals ($\text{M} = \text{V(III)}$, Mn(III) and Fe(III)) [30].

3.1.3. Manganese

No simple $[\text{Mn}(\text{sal})_2]$ complexes of salicylaldoxime type ligands with manganese appear on the Cambridge Database. However, a study of this chemistry has been carried out and one, as yet unpublished, structure determined [12].

Reaction of the monosodium salt of H_2salMe with manganese(II) acetate in water gives a dark green precipitate that can be recrystallised from acetonitrile. This has been formulated as $[\{\text{Mn}(\text{HsalMe})(\text{salMe})\}_4]$ and is shown by X-ray diffraction to consist of discrete tetrameric units. The four manganese atoms of each tetramer are in identical environments and define a flattened tetrahedral arrangement. Each manganese atom is in a pseudo-square pyramidal coordination environment. One has an N_2O_3 coordination sphere while the remaining three have NO_4 donor sets. The monodeprotonated ligands in the structure are bidentate and each coordinates to one of the manganese atoms through the phenolic oxygen and oximic nitrogen. The doubly deprotonated ligands also each chelate one manganese(II) centre through the phenolate oxygen and oximic nitrogen, but in addition the oxime oxygen bridges to an adjacent manganese. There are four hydrogen bonds between the NOH groups of monodeprotonated ligands and the phenolates of monodeprotonated ligands on adjacent manganese ions which further stabilise the tetramer.

Mn(III) complexes containing the *fac*-octahedral capping group Me_3tacn (= 1,4,7-trimethyl-1,4,7-triazacyclononane) have been reported [31]. Both the homonuclear $[(\text{Me}_3\text{tacn})\text{Mn(III)}(\text{salH})_3\text{Mn(III)}]$ and heteronuclear analogues with metal centres, $[\text{Mn(III)}/\text{Fe(III)}]^0$, $[\text{Mn(IV)}/\text{Fe(III)}]^+$, $[\text{Mn(IV)}/\text{Mn(III)}]^+$ show magnetic exchange involving the oximato-bridges between the two metal centres and can be assumed to have structures very similar to that for $[(\text{Me}_3\text{tacn})\text{Fe(III)}(\text{salH})_3\text{Fe(III)}]$ which is shown in Fig. 25.

Another unusual mixed Mn/Fe complex, $[(\text{Me}_3\text{tacn})_2\text{Fe}_2(\text{salH})_2(\mu_3\text{-O})_2(\mu_2\text{-CH}_3\text{CO}_2)_3\text{Mn}_2](\text{ClO}_4)_4$, has been reported with a structure similar to that for the tetranuclear Fe(III) complex shown in Fig. 26 [31]. These mixed metal complexes are discussed in more detail in Section 3.1.9.

3.1.4. Iron

The chemistry of phenolic oximes with iron provides a second commercial application for these ligands. Long chain alkyl substituted versions of these ligands react at mild steel surfaces to give a purple coating which acts as a protective film against corrosion [2]. Relatively little iron coordination chemistry of these ligands has been published. A knowledge of modes of coordination should prove useful in defining the possible modes-of-action as corrosion inhibitors for iron. For iron(III) the simplest binary complex that might be proposed would

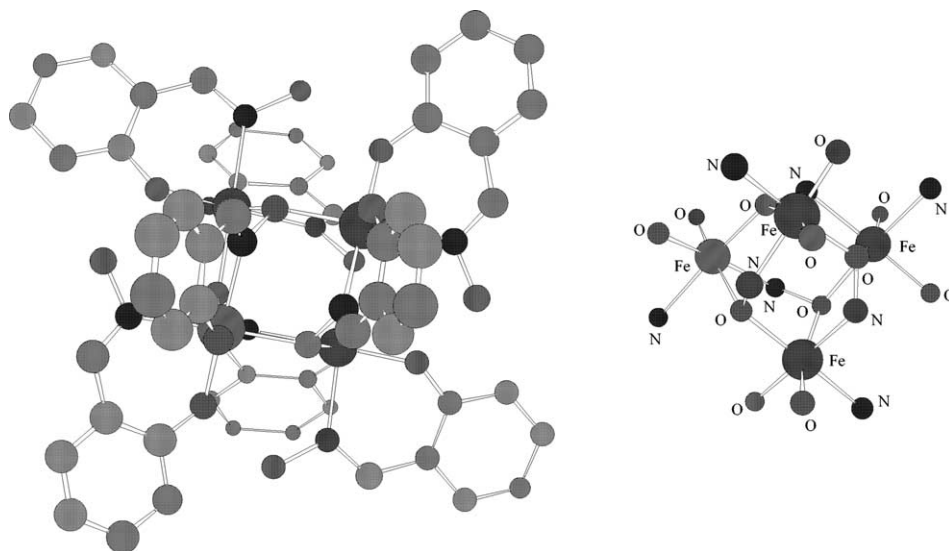


Fig. 24. Solid state structure $[\{\text{Fe}(\text{salH})(\text{HsalH})\}_4]$ together with the tetranuclear cluster showing the coordination sphere of each metal centre. Hydrogen atoms have been excluded for clarity.

be the octahedral $[\text{Fe}(\text{HsalH})_3]$, but it should be noted that no examples of mononuclear ML_3 complexes have been structurally characterised for these systems for any metals. In practice for iron(III) formation of polynuclear complexes is apparently preferred.

The simplest known binary complex is the tetranuclear iron(III) cluster formed from the reaction of iron(III) chloride with H_2salH [2]. The crystalline material formed is formulated as solvated $[\{\text{Fe}(\text{salH})(\text{HsalH})\}_4]$ clusters, Fig. 24. The cluster comprises four Fe(III) centres each of which has a distorted octahedral coordination environment with four O and two *cis* N donor atoms. Each metal centre is coordinated by four different ligands; one bidentate HsalH^- NO donor and four atoms (one N and three O) from three of four bridging salH^{2-} ligands.

In the remaining examples coligands complete the coordination spheres of iron(III) centres in polynuclear complexes. Reaction of ferrous acetate with H_2salH in

methanol, followed by addition of $[(\text{Me}_3\text{tacn})\text{FeCl}_3]$ (Me_3tacn = 1,4,7-trimethyl-1,4,7-triazacyclononane) and triethylamine gives a precipitate and a deep violet solution. The black–brown precipitate has been characterised [31] as $[(\text{Me}_3\text{tacn})\text{Fe}(\text{III})(\text{salH})_3\text{Fe}(\text{III})]$. This dinuclear complex contains an unusual pseudo-octahedral tris-salicylaldiminato unit $[\text{Fe}(\text{salH})_3]^{3-}$ with a facial arrangement of the three oxime nitrogen atoms. The three oxygen atoms of these deprotonated oxime groups define three coordination sites of the other iron atom which is capped by a facial Me_3tacn ligand (Fig. 25).

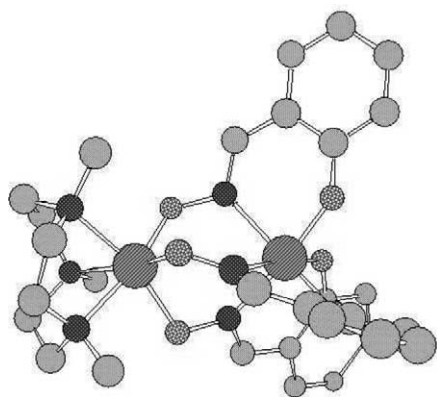


Fig. 25. The solid state structure of $[(\text{Me}_3\text{tacn})\text{Fe}(\text{III})(\text{salH})_3\text{Fe}(\text{III})]$, showing the *fac*-arrangement of the bridging oximato groups in the coordination spheres of both pseudo-octahedral Fe(III) atoms.

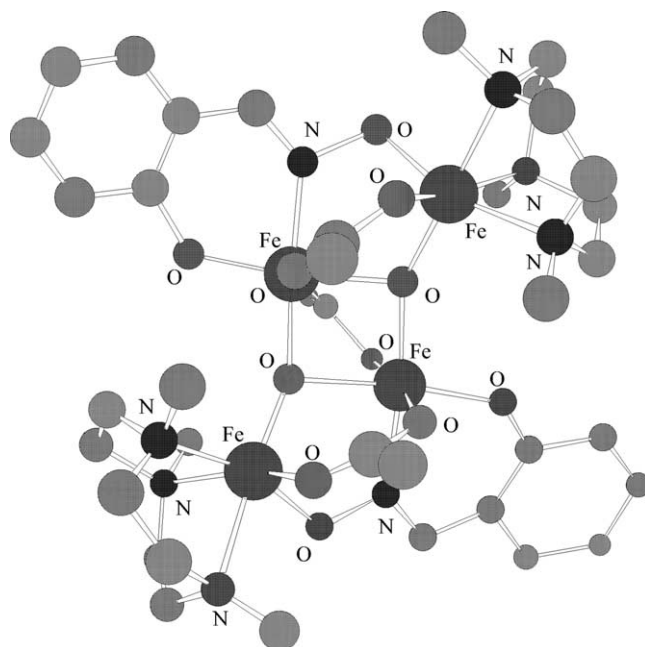
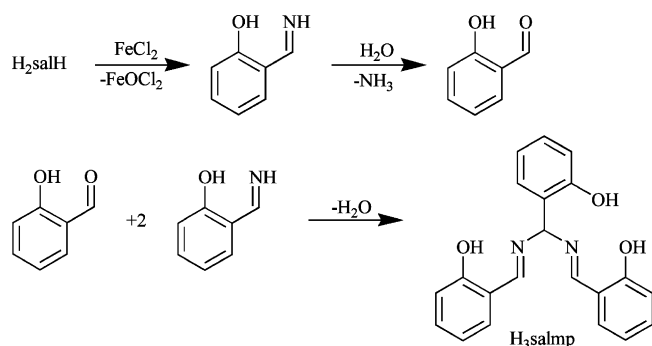
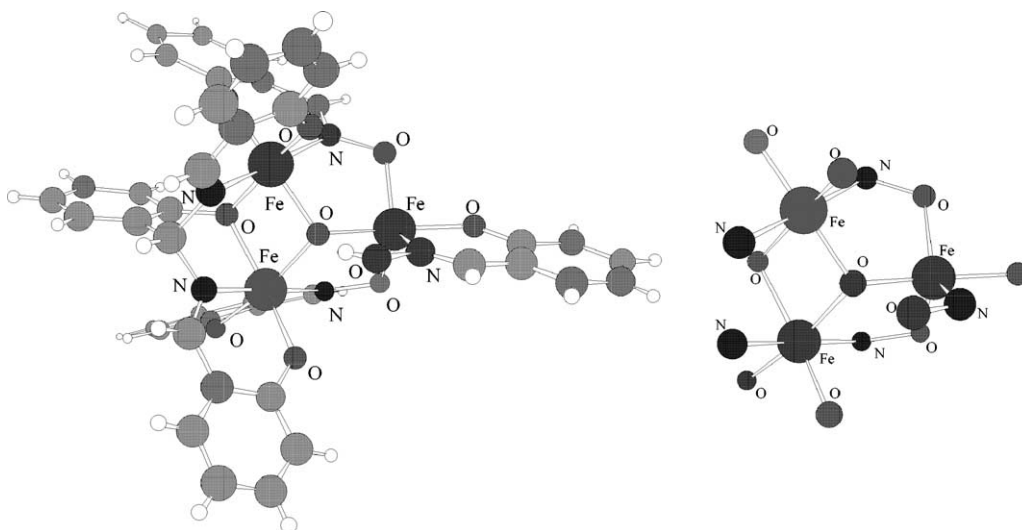
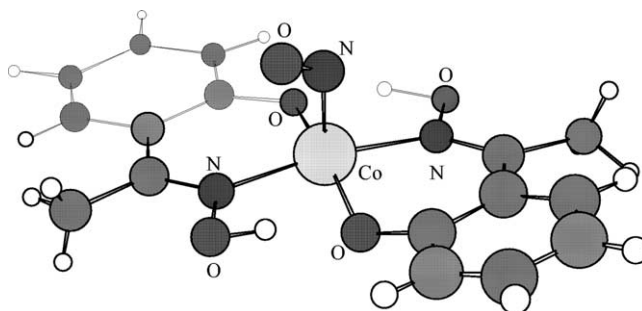


Fig. 26. Solid state structure of $[(\text{Me}_3\text{tacn})_2\text{Fe}_4(\text{salH})_2(\mu_3\text{-O})_2(\mu_2\text{-CH}_3\text{CO}_2)_3]^+$, excluding the hydrogen atoms for clarity.

Scheme 1. Proposed pathway to H₃salmp.

Addition of a perchlorate salt to the violet solution gives dark brown crystals containing [(Me₃-tacn)₂Fe₄(salH)₂(μ₃-O)₂(μ₂-CH₃CO₂)₃](ClO₄), Fig. 26. The structure of the cation is based on a [Fe₄(μ₃-O)₂]⁸⁺ core with a butterfly arrangement of iron atoms based on two edge sharing Fe₃(μ₃-O) units, with a dihedral angle of 154°. Additionally there are three bridging acetates and two bridging –NO groups from deprotonated oximes. Each iron is in a distorted octahedral environment with the two chelated by phenol oxygens having NO₅ coordination while the two coordinated to the macrocycle have N₃O₃ coordination spheres.

Ferrous chloride with H₂salH and triethylamine in methanol under argon gives red brown crystals of [(C₂H₅)₃NH][Fe₃O(HsalH)(salH)₂(salmp)] · 2H₂O, which is isostructural with the V(III) complex formed under similar conditions and is discussed previously in Section 3.1.1, where H₃salmp is the new ligand 2-bis(bis(salicylideneamino)-methyl)phenol [32]. The reaction pathway is proposed to involve the deoxygenation of oxime as outlined in Scheme 1.

Fig. 27. Solid state structure of [Fe₃O(HsalH)(salH)₂(salmp)][−], together with a schematic view of the iron coordination spheres.Fig. 28. Solid state structure [Co(HsalMe)₂(NO)].

This trinuclear complex is based on a [Fe₃(μ₃-O)(μ₂-OPh)]⁶⁺ core. Two irons have pseudo-octahedral N₂O₄ coordination while the third is in a trigonal bipyramidal NO₄ environment. The structure of the complex, together with a diagram describing the iron coordination sphere is given in Fig. 27.

3.1.5. Cobalt

The four phenolic oxime complexes of cobalt in the Cambridge Database all formally contain cobalt(III). Three of these structures are nitrosyl complexes containing the unusual bent nitrosyl ligand. [Co(HsalMe)₂(NO)] [33], [Co(HsalH)₂(NO)] [34] and [Co(5-Cl-HsalH)₂(NO)] [34] all contain five coordinate, square pyramidal cobalt with an apical nitrosyl group (Fig. 28). The basal plane is defined by *trans* bidentate ligands which form a pseudo-macrocyclic motif. The metal lies slightly above this plane (min. 0.15 Å in [Co(HsalH)₂(NO)] and max. 0.24 Å in [Co(HsalMe)₂(NO)]), towards the nitrosyl group. The structural chemistry of these complexes is, therefore, closely related to that with copper where Cu²⁺ is replaced by [CoNO]²⁺. Other structural features of these complexes are summarised in Table 1.

Table 1
Key features of cobalt phenolic oxime nitrosyl complexes

Complex	Nitrosyl			Mean			Ref.
	Co–N (Å)	N–O (Å)	O–N–O (°)	Co–N (Å)	Co–O (Å)	O···O, (Å)	
[Co(HsalH) ₂ (NO)]	1.84(2)	1.48(3)	116(2)	1.86(2)	1.87(1)	2.49	[34]
[Co(HsalMe) ₂ (NO)]	1.91(1)	1.40(1)	113.4(3)	1.91(1)	1.85(1)	2.50	[33]
[Co(5-Cl-HsalH) ₂ (NO)]	1.841(1)	1.070(5)	123.4(3)	1.90(1)	1.87(1)	2.52	[34]

The remaining cobalt(III) complex contains only one phenolic oxime ligand per complex unit [35]. Reaction of *cis*- α -[CoCl₂(trien)]Cl (trien = triethylenetetramine) with silver oxide, potassium hydroxide and H₂salH gives a complex mixture of isomeric materials, one of which has been crystallised. This has been shown to be *cis*- β ₁(RS,SR)-[Co(salH)(trien)]Cl · (acetone) · 2H₂O in which cobalt(III) is coordinated by a doubly deprotonated phenolic oxime ligand and trien. The salH²⁻ ligand binds to cobalt through the phenolic oxygen and oximic nitrogen with bond distances of 1.94(1) and 1.93(1) Å, respectively. There is an intramolecular hydrogen bond between the oxime oxygen and a proton on one of the trien secondary nitrogens with an N···O distance of 2.65(1) Å (Fig. 29).

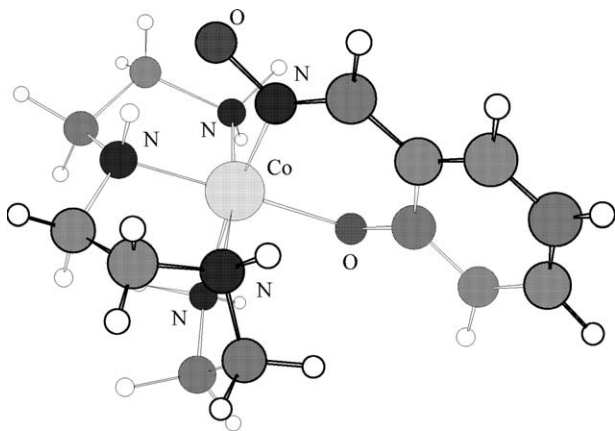


Fig. 29. Solid state structure of [Co(salH)(trien)]Cl.

3.1.6. Nickel

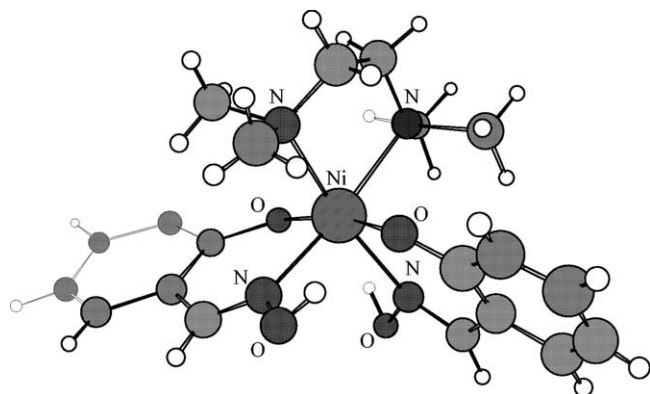
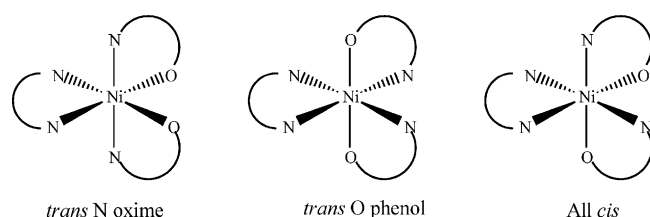
Four binary complexes with nickel have been the subject of structural investigation. All of them, containing the ligands H₂salH, [36] H₂salMe [37] and H₂salEt [38] and 5-Me-H₂salH [39] show typical [ML₂] coordination and in each case hydrogen bonds from the oxime –NOH to the phenolic oxygen stabilise the structures. The H₂salH, H₂salEt and 5-Me-H₂salH complexes are centrosymmetric with the nickel atom lying on a crystallographic inversion centre. By contrast the H₂salMe complex is less symmetrical, with [Ni(HsalMe)₂] having a dihedral angle of 4.27° between the two ligand planes. However, it should be noted that neither of the other complexes is truly planar and all display a small ‘step’ configuration (vide supra). In all cases the nickel is in a slightly distorted square planar geometry. Chelate angles (~92°) are all slightly greater than right angles while non-chelate angles are reduced commensurately to 88°. This reflects the extended bite of the planar six membered N–O chelate of the phenolic oxime. In all cases there are strong interligand hydrogen bonds with O···O distances ca. 2.48 Å and O–H–O angles of 130°.

The reaction of 4-coordinate [Ni(HsalH)₂] type complexes with aliphatic polyamines in aprotic solvents gives new 6-coordinate octahedral nickel(II) complexes of the form [Ni(HsalH)₂(B)] where B represents an aliphatic diamine. Several such complexes have been isolated and characterised crystallographically [13]. Key structural parameters are summarised in Table 2.

The addition of the aliphatic diamine to the coordination sphere forces the phenolic oxime into an arrange-

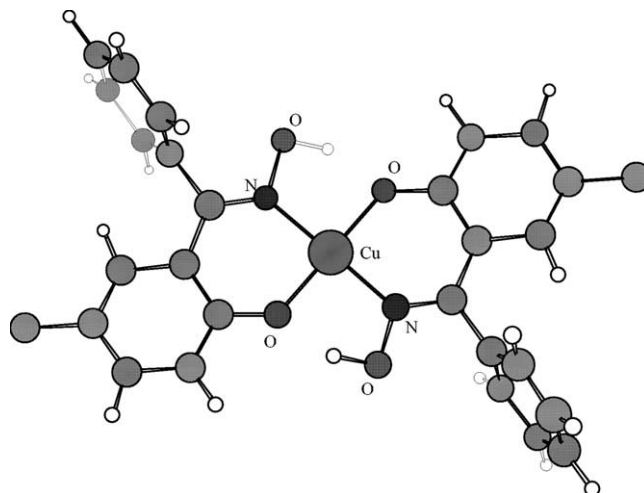
Table 2
Key structural parameters of the nickel(II) phenolic oxime complexes

Complex	Ni–N _(oxime) (Å)	Ni–O _(oxime) (Å)	Ni–N _(amine) (Å)	O···O (Å)	O–Ni–O (°)	N–Ni–N (°)	Ref.
[Ni(HsalH) ₂]	1.855(5)	1.843(5)	n/a	2.520(1)	180.0	180.0	[36]
[Ni(HsalMe) ₂]	1.885(2)	1.817(2)	n/a	2.466(3)	179.21(10)	178.88(9)	[37]
	1.876(2)	1.816(2)		2.479(3)			
[Ni(HsalEt) ₂]	1.884(3)	1.825(2)	n/a	2.483(3)	180.0	180.0	[38]
[Ni(5-Me-HsalH) ₂]	1.887(2)	1.823(2)	n/a	2.470(3)	180.0	180.0	[39]
[Ni(HsalH) ₂ (Me ₄ en)]	2.09(1)	2.09(1)	2.19(1)	2.72	168.7(4)	92.2(5)	[13]
	2.10(1)	2.05(1)	2.16(1)	2.73			
[Ni(HsalH) ₂ (N,N-Me ₂ en)]	2.04(1)	2.012(8)	2.081(10)	2.58	168.9(3)	94.1(4)	[13]
	2.08(1)	2.005(8)	2.204(9)	2.70			
[Ni(HsalH) ₂ (pn)]	2.075(9)	2.047(8)	2.083(9)	2.58	168.5(3)	92.7(4)	[13]
	2.043(10)	2.073(8)	2.09(1)	2.68			

Fig. 30. Solid state structure of $[\text{Ni}(\text{HsalH})_2(\text{Me}_4\text{en})]$.Scheme 2. Possible isomers of $[\text{Ni}(\text{HsalH})_2(\text{B})]$ complexes.

ment with a *cis* configuration of the oxime nitrogen atoms. This allows the intramolecular oxime hydrogen to phenolic oxygen hydrogen bonds to be maintained in the complex unit (see Fig. 30).

On going from the 4-coordinate $[\text{Ni}(\text{HsalH})_2]$ complex to the six coordinate amine adduct the $\text{Ni}-\text{N}_{(\text{ox})}$ bonds lengthen by $\sim 0.3 \text{ \AA}$ and the $\text{Ni}-\text{O}_{(\text{ox})}$ bonds by $\sim 0.25 \text{ \AA}$ leading to an overall increase in the size of the pseudo-macrocyclic inner great ring. This is reflected in an increase in the $\text{O}_{(\text{ox})} \cdots \text{O}_{(\text{phenolate})}$ distance of $\sim 0.2 \text{ \AA}$ which would lead to a corresponding weakening of the interligand hydrogen bonds. It is interesting to note, however, that despite the almost orthogonal arrange-

Fig. 31. Structure of $[\text{Cu}(5\text{-Me-HsalPh})_2] \cdot 2\text{CHCl}_3$. Hydrogen bonded chloroform molecules of crystallisation are omitted for clarity.

ment of the oxime ligands this hydrogen bonding still occurs. Of the three possible isomers that could be formed for $[\text{Ni}(\text{HsalH})_2(\text{B})]$ complexes (Scheme 2) only the *trans-O*-phenol is observed, presumably because it is only in this isomer that the pseudo-macrocyclic hydrogen bonded structure can be preserved.

3.1.7. Copper

Structural parameters are available for comparison for eight of the copper complexes included in Table 3. A common feature is the *trans* square planar coordination of the two ligands around the copper(II) centre, see for example Fig. 31.

The geometry of the cavities presented by the $\text{N}_2\text{O}_2^{2-}$ donor set in the series of complexes can be compared using the parameters in Table 3. The $\text{N} \cdots \text{O}$ bite values in the chelating phenolic oxime units vary less than the $\text{O} \cdots \text{O}$ separations. This implies that steric bulk of the substituents is more readily accommodated by adjust-

Table 3
Selected interatomic distances in the coordination spheres of copper(II) complexes of phenolic oximes

Complex	Cu–O (Å)	Cu–N (Å)	Bite N \cdots O (Å)	O \cdots O (Å)	Hole size (Å)	R_{H}^c	Apical Cu–O (Å) ^b	Ref.
$[\text{Cu}(\text{HsalH})_2]$	1.92(1)	1.94(1)	2.76	2.58(2)	1.93(1)		2.66(1)	[40]
$[\text{Cu}(5\text{-Cl-HsalH})_2]$	1.908(9)	1.957(9)	2.775(14)	2.63	1.932(9)		3.013(10)	[41]
$[\text{Cu}(\text{HsalMe})_2]^a$	1.884(3)	1.958(4)	2.744(7)	2.597(8)	1.920(4)		2.666(5)	[42]
	1.877(3)	1.968(4)	2.726(2)	2.543(7)				
$[\text{Cu}(\text{HsalEt})_2]$	1.882(2)	1.949(2)	2.741(4)	2.58(3)	1.915(3)			[43]
$[\text{Cu}(3\text{-CH}(\text{OMe})_2\text{-5-Me-HsalH})_2]$	1.865(3)	1.946(4)	2.738(5)	2.652(5)	1.905(5)			[44]
$[\text{Cu}(5\text{-Me-HsalH})_2]$	1.914(3)	1.933(4)	2.76	2.59	1.924(5)		2.564	[10]
$[\text{Cu}(3\text{-}^i\text{Bu-5-Me-HsalH})_2]$	1.913(4)	1.934(5)	2.75	2.64	1.924(5)			[10]
$[\text{Cu}(5\text{-Me-HsalPh})_2]$	1.873(5)	1.935(7)	2.74	2.55	1.904(6)	$\text{Cl}_3\text{CH} \cdots \text{O}$	2.03	[10]
Mean	1.839(19)	1.947(12)	2.748(14)	2.60(4)	1.919(10)			

Three entries in the CDS database, for $[\text{Cu}(5\text{-Me-HsalMe})_2]$, $[\text{Cu}(5\text{-Et-HsalMe})_2]$ and $[\text{Cu}(5\text{-Me-HsalEt})_2]$ do not contain positional parameters [16].

^a In this structure the Cu(II) atom does not lie on an inversion centre.

^b Intermolecular contact with a phenolic or oxime oxygen in an adjacent molecule.

^c Defined as mean distance of donor atoms from the centroid [45].

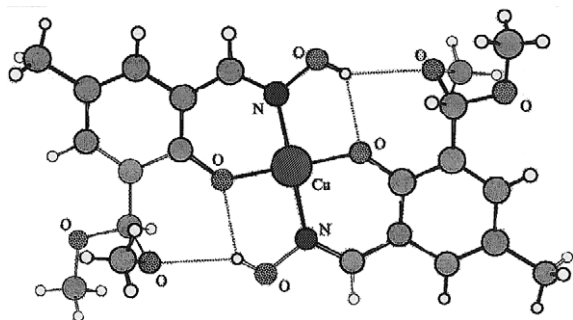


Fig. 32. The bifurcated hydrogen bonding involving the oximic hydrogen and the phenolate oxygen and the methoxy substituent. Distances $O_{\text{oxim}} \cdots O_{\text{phen}}$ $O_{\text{oxim}} \cdots O_{\text{methoxy}}$ are 2.652(5) and 3.033(5) Å, respectively.

ment of the H-bonding component of the pseudo-macrocyclic. The closing down of the circumferences of this part of the system by the phenyl group in $[\text{Cu}(5\text{-Me-HsalPh})_2]$ provides an explanation for this complex having the smallest cavity ($R_{\text{H}} = 1.904(10)$ Å). Introduction of a bulky tertiary butyl group in the 3-position of the aromatic ring (adjacent to the phenol group), as might be expected, leads to an increase in the $O \cdots O$ separation, apparently weakening the hydrogen bond slightly. The effect of this on the overall cavity size is not statistically significant.

Incorporation of a hydrogen bond acceptor substituent, $-\text{CH}(\text{OMe})_2$, in the 3-position in the complex $[\text{Cu}(3\text{-(OMe)}_2\text{-5-Me-HsalH})_2]$ lengthens the $O \cdots O$ distance because a bifurcated hydrogen bond is observed with the oximic OH group aligned to place the hydrogen atom between the phenolic oxygen and the methoxy substituent (see Fig. 32). A consequence of ‘pulling’ the oximic OH towards the methoxy substituent is to decrease the $\text{N}_2\text{O}_2^{2-}$ cavity size to 1.905(5) Å.

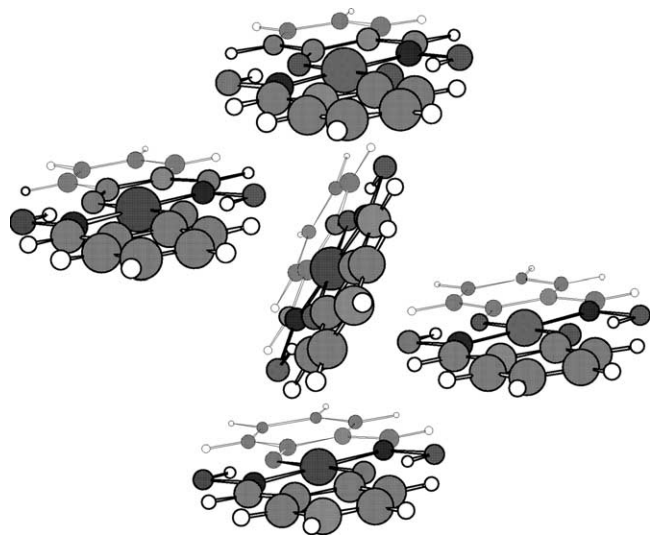


Fig. 33. The two dimensional sheet formed by $[\text{Cu}(\text{HsalH})_2]$ via weak oxime oxygen to Cu(II) interactions (2.66(1) Å). A similar structure is present in $[\text{Cu}(5\text{-Me-HsalH})_2]$ ($\text{Cu} \cdots \text{O}$, 2.56 Å).

For $[\text{Cu}(\text{HsalH})_2]$ and $[\text{Cu}(5\text{-Cl-HsalH})_2]$ we can compare the cavity sizes, 1.93(1) and 1.932(9) Å, respectively, with values of 2.10(1) and 2.08(1) Å in the ‘preorganised’ dimeric free ligands (see Fig. 9). Replacement of the two phenolic protons in the preorganised dimers results in an opening up of the chelate $O \cdots N$ bite from 2.63 and 2.65 to 2.76 and 2.78 Å, respectively, whilst the $O \cdots O$ distances are reduced from 2.82 and 2.83 to 2.58 and 2.63 Å. This shortening of the $O \cdots O$ distances and apparent strengthening of the oximic OH to phenolate oxygen hydrogen bond helps to account for this class of reagents being ‘strong’ extractants for copper(II). The donor–donor repulsion enthalpies associated with bringing together separate ligands into the coordination sphere of a metal ion are compensated by formation of the favourable ligand:ligand hydrogen bonds. Selectivity of formation of copper(II) complexes over other divalent planar transition metal ions could be related to the particularly good fit of copper(II) into the $\text{N}_2\text{O}_2^{2-}$ cavity. An analysis of the goodness-of-fit [45] is difficult for copper(II) because the plasticity of the coordination sphere makes it impracticable to define effective covalent radii of this metal ion with particular donor atom types.

The copper atoms are required to be strictly in the $\text{N}_2\text{O}_2^{2-}$ coordination planes of all but one of the structures as a consequence of their inversion centres. The packing of the complexes appears to be dominated by the requirement for copper to form weak interactions in its apical sites to oxygen atoms in adjacent units leading to highly tetragonally distorted octahedral or square pyramidal geometries. In $[\text{Cu}(\text{HsalH})_2]$ and $[\text{Cu}(5\text{-Me-HsalH})_2]$ each copper makes two interactions with oximic oxygens on adjacent molecules giving the two dimensional layer structure leading to tetragonally distorted copper(II) centres as illustrated in Fig. 33.

In $[\text{Cu}(5\text{-Cl-HsalH})_2]$ the copper(II) centres associate with phenolic oxygens on adjacent units ($\text{Cu} \cdots \text{O}$, 3.01 Å), generating highly tetragonally distorted 6-coordi-

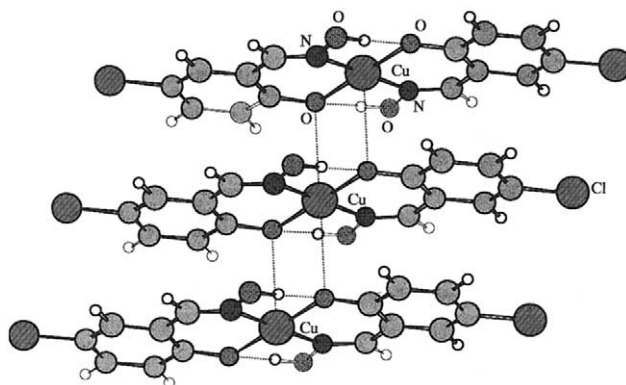


Fig. 34. The one dimensional ribbon formed by $[\text{Cu}(5\text{-Cl-HsalH})_2]$ in the solid state.

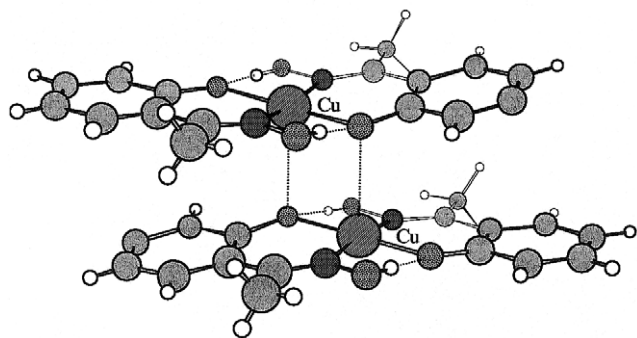


Fig. 35. The dimeric structure of $[\text{Cu}(\text{HsalMe})_2]$ formed in the solid state, showing the distorted square pyramidal geometry at Cu (apical $\text{Cu}\cdots\text{O}$, 2.666(5) Å).

nate copper atoms in one dimensional ribbons [41] (see Fig. 34).

The copper atoms in $[\text{Cu}(\text{HsalMe})_2]$ also associate with phenolic oxygens via a co-facial approach of complex units, but in this case only dimers are formed (see Fig. 35), probably because the bulky methyl substituents restrict efficient packing, therefore, destabilising the formation of ribbons.

The introduction of bulky groups into the ligands prevents the close approach of the complexes that is required to produce the apical interaction which give rise to these structural motifs. Therefore, in $[\text{Cu}(\text{HsalEt})_2]$, $[\text{Cu}(3\text{'-Bu-5-Me-HsalH})_2]$ and $[\text{Cu}(5\text{-Me-HsalPh})_2]$ no intermolecular coordination sphere contacts are observed and the complexes remain as discrete molecular species. The breaking down of such inter-complex interactions has important consequences in providing good solubility in the hydrocarbon solvents which are used in commercial operations to recover copper using such phenolic oxime ligands (see Section 1.1).

One further complex of note is that of 5-Me- H_2salPh which provides the only example of the oxime oxygen acting as a hydrogen bond acceptor. In this case a chloroform of crystallisation occupies cavities formed within the structure by the staggered orientation of the phenyl rings and are orientated by hydrogen bonding ($\text{O}\cdots\text{H}$ 2.03 Å). These chloroform molecules are tenu-

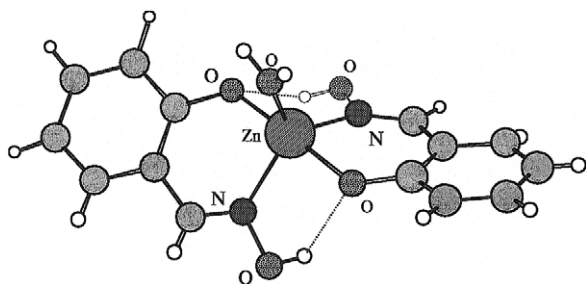


Fig. 36. Solid state structure of $[\text{Zn}(\text{HsalH})_2(\text{H}_2\text{O})]$.

ously bound in the crystals, and on standing they decompose with loss of the solvent.

3.1.8. Zinc

Two zinc(II) structures are available for analysis. Preparation of the complex from hydrated zinc acetate in methanol yields [46] the monoaquo complex $[\text{Zn}(\text{HsalH})_2(\text{H}_2\text{O})]$ which on recrystallisation from chloroform gives the dimeric complex $[(\text{Zn}(\text{HsalH})_2)_2]$ [11]. In the aquo complex $[\text{Zn}(\text{HsalH})_2(\text{H}_2\text{O})]$ the zinc atom has a distorted trigonal bipyramidal geometry with the water molecule occupying an equatorial position (Fig. 36). The two oximic nitrogens and the water are coplanar with zinc (the sum of angles in the equatorial plane is 360.0°) and the two axial zinc-phenolic oxygen bonds are of the same length and almost colinear ($\text{Zn}-\text{O}$, 2.041(4) and 2.047(4) Å; $\text{O}-\text{Zn}-\text{O}$, $172.7(2)^\circ$). The HsalH^- ligands are planar and, although inclined at an angle of 45° with respect to each other, are still able to form a pseudo-macrocyclic motif with strong phenolate-oxime hydrogen bonds ($\text{O}\cdots\text{O}$, 2.778(8) and 2.749(5) Å). In addition the phenolate oxygens form intermolecular hydrogen bonds to waters in adjacent molecules to produce infinite linear chains which are linked by weaker hydrogen bonds to form layers.

In $[(\text{Zn}(\text{HsalH})_2)_2]$ each zinc atom in the dimer is coordinated to two bidentate salicylaldoximate ligands. Both bind zinc through the oximic nitrogen and phenolic oxygen but for one of the ligands the oxygen acts in a μ_2 fashion binding to a neighbouring, similarly coordinated zinc. This produces a centrosymmetric, dimeric molecule. Each zinc is pentacoordinate and the coordination polyhedron is best described as distorted trigonal bipyramidal. The equatorial positions are occupied by two oximic nitrogens ($\text{Zn}-\text{N}$, 2.030(4) and 2.015(5) Å) and a bridging phenolate oxygen ($\text{Zn}-\text{O}$, 2.071(3) Å), all of which are coplanar with the zinc (the sum of angles around the zinc equatorial plane is 359.5°). The axial positions are occupied by a terminal phenolate at 1.965(4) Å and a further bridging phenolate at 2.077(3) Å. The $\text{Zn}-\text{O}$ distances are, therefore, very similar and the $\text{Zn}-\text{O}-\text{Zn}$ angle is $96.7(1)^\circ$ giving a $\text{Zn}-\text{Zn}$ separation of 3.100(2) Å. The whole structure is further stabilised by intramolecular hydrogen bonds between oximic hydrogens and phenolates.

3.1.9. Mixed first row transition metal complexes

Two isostructural mixed metal complexes of the ligand H_2salH have been reported, both of which incorporate chromium.

The first example, $[(\text{Me}_3\text{tacn})_2\text{Cr}_2(\text{OMe})_2(\mu_3\text{-O})_2(\text{sal-H})_2\text{Fe}_2](\text{ClO}_4)_2 \cdot 3\text{H}_2\text{O}$ was prepared by the reaction of $[(\text{Me}_3\text{tacn})\text{Cr}(\text{MeOH})_3]^{3+}$ with H_2salH and $[\text{Fe}(\text{MeCO}_2)_2]$ in methanol, followed by precipitation of the product with perchlorate [47]. The second

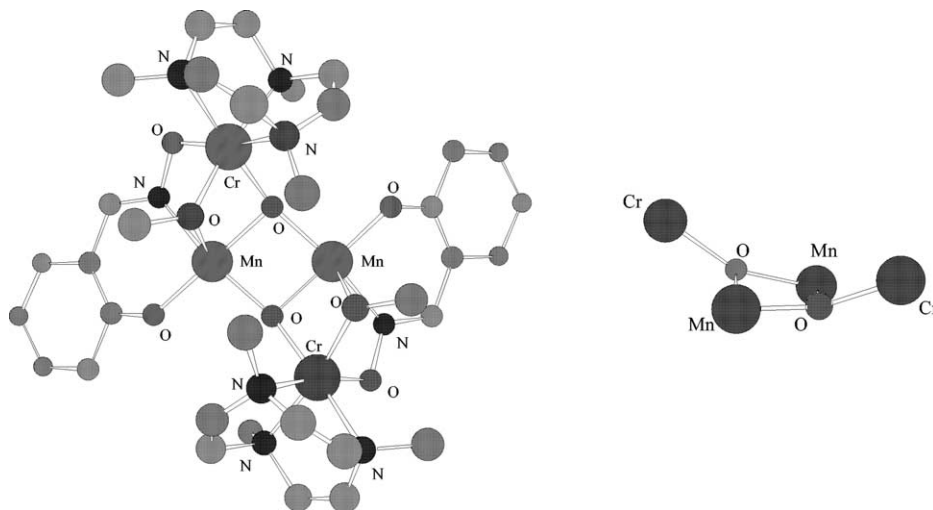


Fig. 37. Structure of $[(\text{Me}_3\text{tacn})_2\text{Cr}_2(\text{OMe})_2(\mu_3\text{-O})_2(\text{salH})_2\text{Mn}_2]^{2+}$ with the perchlorate anion and hydrogens excluded for clarity, together with the oxygen capped butterfly structure of the $[\text{Cr}_2(\text{III})\text{Mn}_2(\text{III})(\mu_3\text{-O})_2]^{6+}$ core.

example is prepared in an analogous fashion, but replacing iron(II) acetate with manganese(III) acetate [48]. The two compounds are isostructural and only the manganese complex will be discussed in detail here.

The cation, shown in Fig. 37, is symmetric and has a two-fold rotation axis. It is based on a $[\text{Cr}_2(\text{III})\text{Mn}_2(\text{III})(\mu_3\text{-O})_2]^{6+}$ core, which has an oxygen capped butterfly structure.

Geometric parameters for both the manganese and iron compounds are given in Table 4. Of note is the short $\text{Mn}\cdots\text{Mn}$ and $\text{Fe}\cdots\text{Fe}$ interactions observed in both compounds. The coordination geometry of the N_3O_3 donor sets around the chromium atoms is *fac*-octahedral. Three nitrogens of the triaza macrocycle coordinate confacially, while the remaining coordination sites are occupied by oxygen atoms from the μ_3 -oxo, a bridging methoxide and from the deprotonated oxime group. The primary coordination of the manganese is square based pyramidal, however, there is a weak interaction with a water molecule ($\text{Mn}\cdots\text{O}$, 2.79 Å) giving overall pseudo-octahedral coordination. Considerable tetragonal distortion is seen for the manganese atoms and the axial $\text{Mn}\text{--O}$ distance of 2.20 Å, occupied by the bridging methoxide, is considerably longer than bond distances seen for the equatorial atoms. The equatorial plane of the manganese coordination sphere

is formed by two μ_3 -oxygen atoms and by the phenol oxygen and oxime nitrogen of the chelating $(\text{salH})^{2-}$ ligand.

3.2. Second and third row transition metals

3.2.1. Molybdenum

Only one structure of a phenolic oxime with molybdenum has been determined. On reaction of

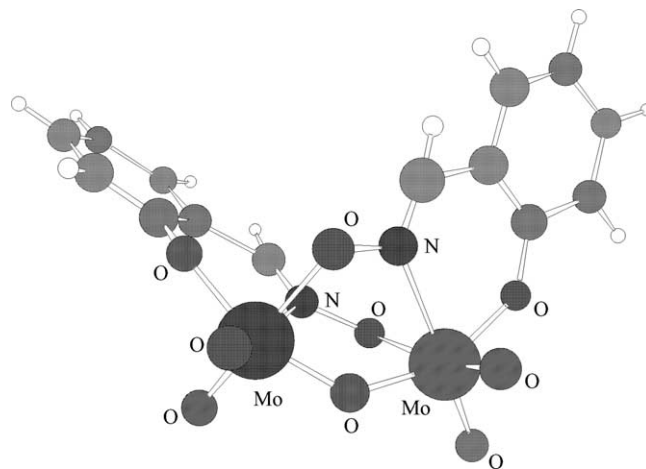


Fig. 38. Solid state structure of $[\text{Mo}_2\text{O}_5(\text{salH})_2]^{2-}$. The location of the azomethine H-atom appears to be incorrectly reported [49].

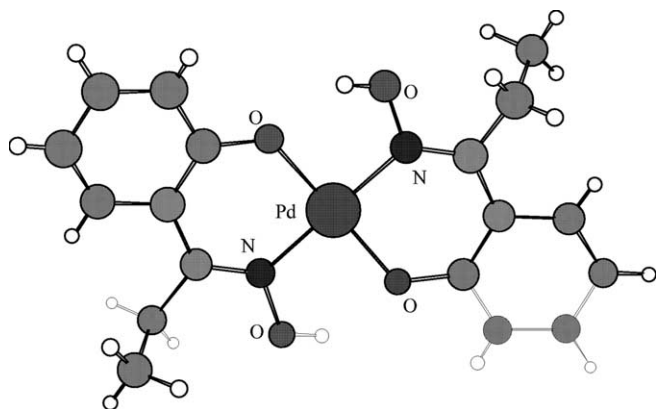
Table 4

Geometric parameters for the isostructural manganese(III) and iron(III) complexes with HsalH_2

Compound ^a	$(\text{salH})^{2-}$			$\text{Cr}\cdots\text{Cr}$ (Å)	$\text{M}\cdots\text{M}$ (Å)	$\text{M}\text{--O}\text{--M}$ (°)	Dihedral angle (°) ^b	Ref.
	$\text{Cr}\text{--O}$ (Å)	$\text{M}\text{--O}$ (Å)	$\text{M}\text{--N}$ (Å)					
$[\text{Cr}_2(\text{III})\text{Fe}_2(\text{III})(\mu_3\text{-O})_2]^{6+}$	1.954(20)	1.884(17)	1.979(21)	5.66	2.736(10)	93.2(5)	135.3	[47]
$[\text{Cr}_2(\text{III})\text{Mn}_2(\text{III})(\mu_3\text{-O})_2]^{6+}$	1.931(12)	1.857(11)	2.025(14)	5.664(3)	2.742(7)	94.2(3)	135.4	[48]

^a $\text{M} = \text{Fe}$ and Mn for $[\text{Cr}_2(\text{III})\text{Fe}_2(\text{III})(\mu_3\text{-O})_2]^{6+}$ and $[\text{Cr}_2(\text{III})\text{Mn}_2(\text{III})(\mu_3\text{-O})_2]^{6+}$, respectively.

^b The dihedral angle is the angle between two planes defined by the $\text{CrM}_2(\mu_3\text{-O})$ triangular units, where $\text{M} = \text{Fe}$ or Mn .

Fig. 39. Solid state structure of $[\text{Pd}(\text{HsalEt})_2]$.

$[(\text{C}_4\text{H}_9)_4\text{N}]_2[\text{Mo}_2\text{O}_7]$ with H_2salH , yellow crystals of the molybdenum(VI) complex $[(\text{C}_4\text{H}_9)_4\text{N}]_2[\text{Mo}_2\text{O}_5(\text{salH})_2]$ are obtained [49]. The X-ray structure determination shows that in this dimolybdenum complex, two *cis* dioxomolybdenyl centres are bridged by an oxo group and by the deprotonated oxime groups from two ligands, each binding in a μ_2 mode. Geometrical parameters are consistent with sp^2 hybridization of the oximato nitrogen with double bond character localised along the C–N bond. This two atom bridge between the molybdenum centres requires the Mo–O–Mo angle to expand to 132° compared with the usual $\sim 110^\circ$ seen with single atom bridges. The pseudo-octahedral NO_5 coordination sphere of each molybdenum is completed by a phenolate oxygen from one of the ligands (Fig. 38).

3.2.2. Palladium

The coordination chemistry of palladium(II) with phenolic oxime ligands is closely related to that of copper. Of the three reported structure determinations, that for $[\text{Pd}(\text{5-Cl-HsalH})_2]$ gives [50] only the unit cell dimensions and space group. The two complete structures $[\text{Pd}(\text{HsalH})_2]$ [51] and $[\text{Pd}(\text{HsalEt})_2]$ [52] show *trans* planar coordination of two monodeprotonated ligands to a square planar palladium(II) centre forming a pseudo-macrocyclic complex (see Fig. 39). The N–Pd–O chelate angles are slightly greater than 90° , a feature also seen for the nickel(II) complexes, reflect the relatively small bite angle (even for a late transition element) of the six membered ligand chelate. Other structural features are given in Table 5.

Table 5

Key features of palladium phenolic oxime complexes.

Complex	Pd–N (Å)	Pd–O (Å)	O–Pd–N (°) chelate	O–Pd–N (°) non-chelate	O···O (Å)	Ref.
$[\text{Pd}(\text{HsalH})_2]$	1.96(1)	1.98(1)	92.5(7)	87.5(7)	2.62(2)	[51]
$[\text{Pd}(\text{HsalEt})_2]$	1.979(3)	1.970(2)	92.2(1)	87.8(1)	2.594(5)	[52]

3.2.3. Platinum

Two platinum complexes have been structurally characterised with the phenolic oxime moiety. Unlike the palladium(II) complexes, which are similar in coordination chemistry to that of nickel(II) and copper(II) in that they form mononuclear bis-bidentate species, both the platinum complexes coordinate to only one phenolic oxime. On reaction of $\text{K}[\text{Pt}(\text{Cl})_3(\text{Me}_2\text{SO})]$ with H_2salH , in ethanol, a yellow platinum(II) complex $[\text{Pt}(\text{Cl})_2(\text{H}_2\text{salH})(\text{Me}_2\text{SO})]$ is obtained with the oxime bound in a monodentate fashion. In the presence of one equivalent KOH, under analogous conditions, the phenolic oxygen is deprotonated leading to the formation of both the *cis*-(*S,N*)- and *trans*-(*S,N*)- $[\text{Pt}(\text{Cl})(\text{HsalH})(\text{Me}_2\text{SO})]$ complex [53]. The X-ray structure of the *cis*-(*S,N*)-isomer has been determined, Fig. 40(a). The platinum is arranged in a planar geometry with the dimethylsulfoxide oxygen lying in the same plane. The geometry is stabilised with an intramolecular hydrogen bond between the oximic hydrogen and the dimethylsulfoxide oxygen (O···O, 2.578(8) Å).

Treatment of *trans*-(*S,N*)- $[\text{Pt}(\text{Cl})(\text{HsalH})(\text{Me}_2\text{SO})]$ as a chloroform solution with excess Cl_2 results in oxidative addition of chlorine to the platinum(II) centre and chlorination of the benzene ring at *ortho* and *para* positions to afford the platinum(IV) *trans*-(*S,N*)- $[\text{Pt}(\text{Cl})_3(3,5\text{-diCl-HsalH})(\text{Me}_2\text{SO})]$ complex, [53] Fig. 40(b). The platinum(IV) centre is 6-coordinate with a slightly distorted octahedral *mer*-geometry with respect to the chlorides. As in the platinum(II) complex the dimethylsulfoxide oxygen lies in the same plane as the PtSNOCl atoms with an additional intramolecular interaction between the oximic hydrogen and the equatorial chlorine (O···Cl, 3.03 Å) reinforcing the stability of the *trans* geometry.

3.3. Complexes of other elements

3.3.1. Boron

X-ray structures of two phenolic oxime boron complexes have been reported. Diphenylborinic acid reacts with H_2salH to give a colourless product formulated as $[(\text{salH})\text{BPh}]_2$, shown schematically together with the complete structure in Fig. 41 [54]. The boron atoms in the structure are chiral and a racemic mixture of *RR* and *SS* forms crystallise from acetone solution. The molecule comprises of a linear but non-planar system of five fused six membered rings. A central $\text{B}_2\text{N}_2\text{O}_2$ ring which

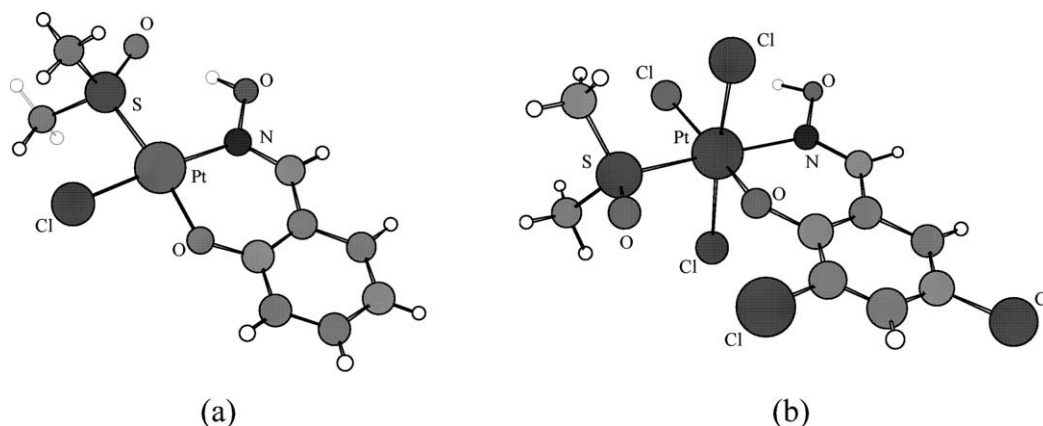


Fig. 40. Solid state structures of (a) *cis*-(*S*, *N*)-[Pt(Cl)(HsalH)(Me₂SO)] and (b) [Pt(3,5-diCl-HsalH)(Cl)₃(Me₂SO)].

has a distorted boat conformation is flanked by two C₃BNO rings which in turn are fused to the aromatic C₆ rings of the phenolic oxime ligands. The overall molecule has approximate C₂ symmetry and the boron atoms are tetrahedrally coordinated. The PhB unit (B–C, 1.596(2) Å) is chelated by the salH^{2–} ligands through the phenolic oxygen and oximic nitrogen atoms (B–O, 1.467(2) Å; B–N, 1.599(2) Å). The final coordination site is occupied by an oximic oxygen from the adjacent ligand (B–O, 1.472(2) Å) leading to dimer formation. The chelating O–B–N angle is 104.6(1)° demonstrating the large ligand bite angle possible with the small boron atom.

Reaction of oxybis(diphenylborane) with H₂salH gives rise to a second boron complex formulated as [(HsalH)BPh₂] [55]. Bond lengths and angles in the H₂salH ligand are very similar to those seen in the [(HsalH)BPh]₂ complex and the structure can be described in terms of replacing the ‘chelated’ proton from the ligand with a diphenylborenyl cation. The BPh₂ unit is, therefore, chelated by the HsalH[–] ligand (B–O, 1.516(1) Å; B–N, 1.609(2) Å) but the chelate ring is non planar and adopts a half chair conformation. The coordination geometry at boron closely approximates

to ideal tetrahedral. Intermolecular hydrogen bonding is a feature of the structure with a strong interaction between the phenolic oxygen and an oximic OH on an adjacent molecule. This results in a spiralling one dimensional polymer chain through the crystal which is closely related to the one dimensional polymers seen for the free ligands. This hydrogen bonded polymer is shown in Fig. 42, together with the structure of a single [(HsalH)BPh₂] molecule.

3.3.2. Gallium

A single solid state structure of gallium with a phenolic oxime ligand has been reported. Reaction of H₂salH with trimethyl gallium in tetrahydrofuran gives pale yellow crystalline plates which have been structurally characterised as the relatively unusual 5-coordinate complex, [GaMe(HsalH)₂] Fig. 43 [56]. The coordination geometry at gallium is distorted square pyramidal and the molecule has crystallographically imposed C₂ symmetry. However, there is disorder in the gallium bound methyl group, which is free to rotate. The basal plane of the square pyramid is formed by the two mono deprotonated phenolic oxime ligands which are linked by strong oxime OH to phenolate oxygen hydrogen

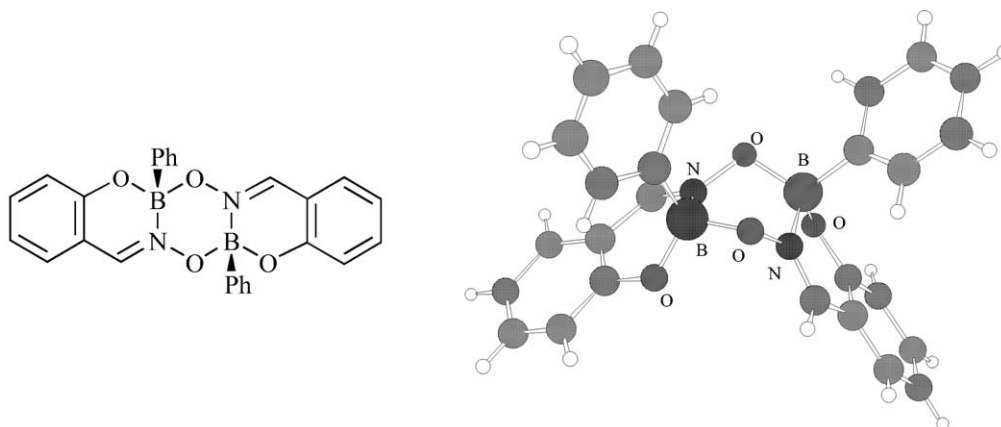


Fig. 41. Solid state structure of [(salH)BPh₂].

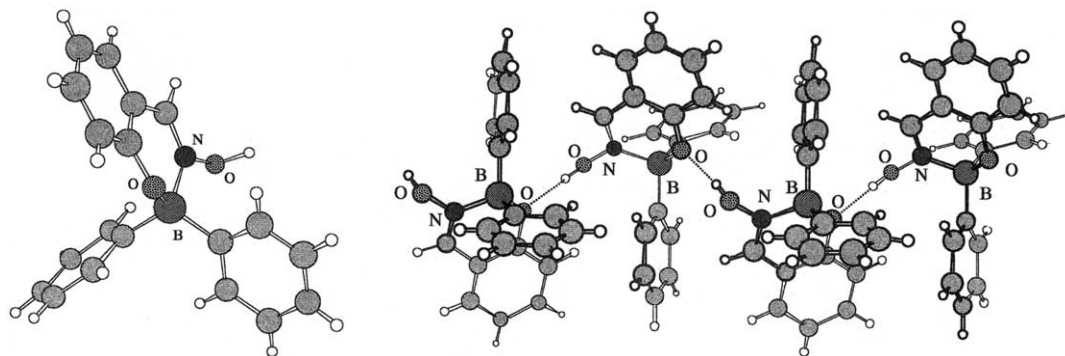


Fig. 42. Structure of [(HsalH)BPh₂] monomer and the one dimensional hydrogen bonded polymer it forms in the solid state.

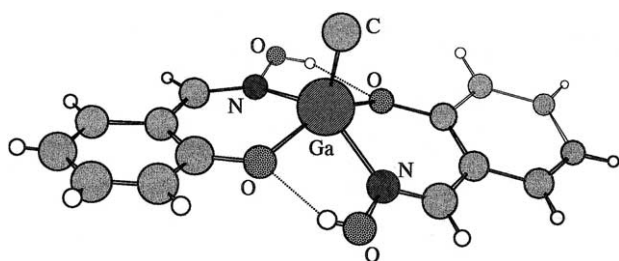


Fig. 43. Solid state structure of [GaMe(HsalH)₂].

bonds (O···O, 2.571(3) Å; O–H–O, 146(4)° giving a reported hydrogen bond length of 1.96(3) Å). The gallium is displaced by 0.7068(4) Å from the mean N₂O₂ basal plane of the donor set toward the carbon of the methyl group (Ga–C, 1.947(5) Å). This results in both chelating and non-chelating N–Ga–O angles being acute (chelating O–Ga–N, 84.94(7)°, non-chelating O–Ga–N, 80.91°). The complex, therefore, represents yet another example of the pseudo-macrocyclic motif characteristic of phenolic oxime chemistry.

3.3.3. Tin

Eleven closely related structures of phenolic oxime complexes of tin appear on the Cambridge Structural

Database. Structural data for all eleven related compounds are given in Table 6.

Reaction of di-*n*-butyl tin oxide with H₂salH gives a crystalline product which has been formulated by X-ray

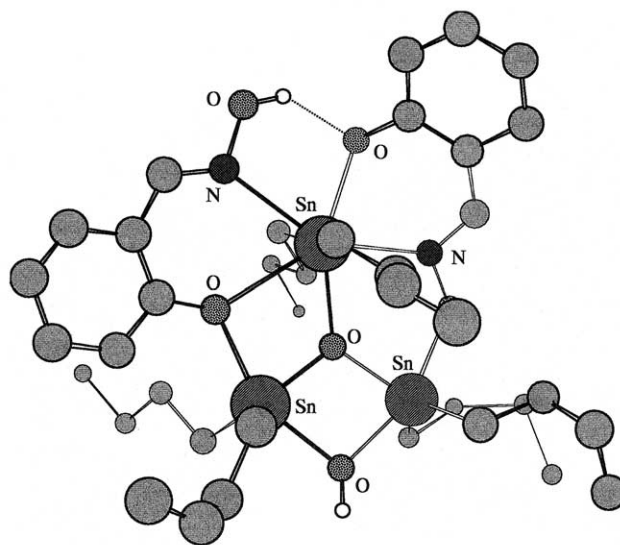
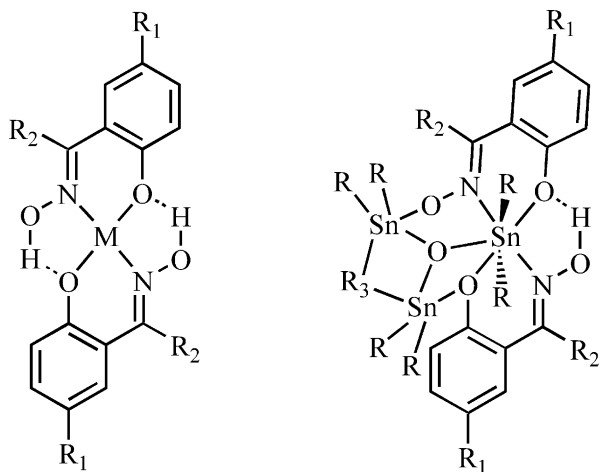


Fig. 44. Solid state structure of [(Bu₂Sn)(Bu₂SnO)(Bu₂SnOH)(HsalH)(salH)] excluding the hydrogen atoms for clarity.

Table 6

Key features of tin phenolic oxime complexes of the type [(R₂Sn)(R₂SnO)(R₂SnX)(HsalH)(salH)]

R group	X group	HsalH [−]			salH ^{2−}			Sn–O (Å)	O···O (Å)	Ref.
		Sn–N (Å)	Sn–O (Å)	N–Sn–O (°)	Sn–N (Å)	Sn–O (Å)	N–Sn–O (°)			
<i>n</i> Bu	HO	2.67(1)	2.68(1)	66.2(7)	2.29(1)	2.26(1)	76.7(5)	2.14(1)	2.572(19)	[57]
Me	MeO	2.588(7)	2.661(5)	66.3(2)	2.313(6)	2.189(5)	75.9(2)	2.170(5)	2.592(7)	[58]
Me	EtO	2.603(6)	2.678(5)	65.9(2)	2.307(6)	2.198(5)	78.0(2)	2.175(4)	2.544(8)	[58]
Me	<i>n</i> PrO	2.593(7)	2.681(5)	66.1(2)	2.286(7)	2.174(6)	77.8(3)	2.173(5)	2.531(9)	[58]
Me	<i>i</i> PrO	2.60(1)	2.647(5)	66.5(3)	2.33(1)	2.192(8)	76.7(3)	2.170(7)	2.527(12)	[58]
Me	<i>p</i> -BrC ₆ H ₄ O	2.632(7)	2.688(4)	64.76(19)	2.324(5)	2.184(7)	77.7(2)	2.181(4)	2.558(8)	[59]
Me	<i>p</i> -MeC ₆ H ₄ O	2.644(6)	2.695(4)	64.95(17)	2.337(5)	2.191(6)	77.7(2)	2.178(3)	2.541(7)	[59]
Me	PhCHNO	2.628(5)	2.715(4)	65.09(16)	2.332(5)	2.177(5)	77.38(19)	2.177(4)	2.588(7)	[59]
Me	Et(Me)CHCH ₂ O	2.543(6)	2.634(4)	67.6(2)	2.291(5)	2.193(4)	75.1(2)	2.171(4)	2.587(7)	[60]
Me	<i>o</i> -HOC ₆ H ₄ CHNO	2.614(6)	2.730(4)	65.40(14)	2.282(5)	2.186(4)	77.35(16)	2.191(4)	2.592(6)	[61]
Me	F	2.573(1)	2.706(11)	66.7(3)	2.306(12)	2.169(11)	77.1(4)	2.206(11)	2.616(13)	[61]



Scheme 3. A pictorial representation of the relationship between pseudo-macrocyclic complexes and the tin complex.

diffraction as $[(\text{Bu}_2\text{Sn})(\text{Bu}_2\text{SnO})(\text{Bu}_2\text{SnOH})(\text{HsalH})(\text{salH})]$ (Fig. 44) [57].

The complex is a trinuclear tin species and contains one monoanionic $(\text{HsalH})^-$ and one dianionic $(\text{salH})^{2-}$ ligand, each of which coordinates in a tridentate fashion. Both ligands chelate a central tin atom which has overall distorted pentagonal bipyramidal geometry with *n*-butyl groups occupying the axial sites ($\text{C}-\text{Sn}-\text{C}$, $160.0(7)^\circ$). The ligands bind through the phenolic oxygen and oximic nitrogen atoms ($(\text{HsalH})^-$: $\text{Sn}-\text{O}$, $2.68(1)$ Å; $\text{Sn}-\text{N}$, $2.67(1)$ Å; $\text{N}-\text{Sn}-\text{O}$, $66.2(7)^\circ$, $(\text{salH})^{2-}$: $\text{Sn}-\text{O}$, $2.26(1)$ Å; $\text{Sn}-\text{N}$, $2.29(1)$ Å; $\text{N}-\text{Sn}-\text{O}$, $76.7(5)^\circ$). The remaining proton on the $(\text{HsalH})^-$ ligand forms a strong hydrogen bond with the phenolate of the doubly deprotonated ligand ($\text{O}\cdots\text{O}$, $2.57(2)$ Å). The other two tin atoms have distorted trigonal bipyramidal coordination geometries. They are linked by a bridging hydroxyl group and connected to the chelated tin by a tricoordinate O^{2-} anion that lies at the centre of a Sn_3 triangle. In addition one tin is coordinated to the deprotonated oxime oxygen of the $(\text{salH})^{2-}$ ligand and the other to the phenolate of the $(\text{HsalH})^-$ ligand. The structure is, on detailed inspection, closely related to the pseudo-macrocyclic hydrogen bonded systems seen for many phenolic oxime complexes. This relationship is demonstrated in Scheme 3.

Reaction of dimethyl tin oxide with H_2salH in ethanol/toluene gives very similar compounds [58]. The product is almost identical to that described above but with methyl rather than butyl substituents attached to tin. In addition, depending on the alcohol solvent of recrystallisation, the bridging OH^- between the two trigonal pyramidal tins is replaced with the alkoxide of that alcohol. In this way the compounds $[(\text{Me}_2\text{Sn})(\text{Me}_2\text{SnO})(\text{Me}_2\text{SnX})(\text{HsalH})(\text{salH})]$, $\text{X} = \text{OMe}$, OEt , $O^i\text{-Pr}$ and $O^n\text{-Pr}$ can be formed. Further, the methoxide bridged compound reacts with *p*-cresol or *p*-bromophenol and benzaldehyde oxime to replace the methoxide

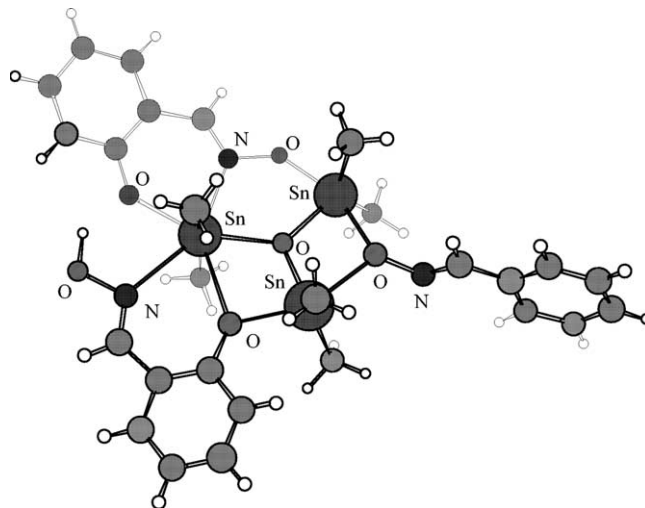


Fig. 45. Solid state structure of $[(\text{Me}_2\text{Sn})(\text{Me}_2\text{SnO})(\text{Me}_2\text{SnX})(\text{HsalH})(\text{salH})]$, $\text{X} = (\text{PhCH}=\text{NO})$.

bridge with a phenoxide or benzaldoximate bridge (Fig. 45) [59]. Similarly reaction with chiral 2-methyl-1-butanol gives the 2-methylbutoxy bridge [60]. A feature of these complexes is the μ_3 -oxo-bridged unit similar to that found in V(III) and Fe(III) complexes (see Sections 3.1.1 and 3.1.4).

One example has been characterised where the μ_2 -bridging group is not oxygenated but rather replaced with an intramolecularly μ_2 -bridged fluoride ligand [61] by the reaction of ammonium fluoride with the methoxide bridged species [62]. A recent review provides an excellent comparison between solid state structures and those in solution as defined by NMR [63].

4. Table's of phenolic oxime ligands and metal complexes

Tables 7 and 8.

5. Summary and conclusions

This survey has confirmed that a wide range of structural types is observed in the coordination chemistry of phenolic oximes. Formation of polynuclear metal complexes is prevalent with the early transition elements, particularly in medium or high oxidation states. This is facilitated by μ -oxo bridging involving oximate or phenolato oxygen atoms in the doubly deprotonated ligands.

A dominant feature in the structures of both the free ligands and their metal complexes is the formation of hydrogen bonds between oximic hydrogen and phenolic oxygen atoms. The formation of pseudo-macrocyclic units by such intramolecular head-to-tail hydrogen bonding in 2:1 complexes with copper goes some way

Table 7

List of known phenolic oxime ligand structures

Ligand	Chemical name	Structural type / features	CCDC code	Ref.
	2-hydroxybenzaldehyde oxime	Dimer [(LH) ₂] ^a O...O = 2.82 ^b O...N = 2.63 ^c R _H = 2.10(1)	SALOXM	[15]
		Positional paras not provided	SALOXM01	[14]
	5-tert-butyl-2-hydroxybenzaldehyde oxime	Polymer [(LH) _n] ^a O...O = 2.78 ^b O...N = 2.62	Unpublished	[11]
	5-tert-octyl-2-hydroxybenzaldehyde oxime	Polymer [(LH) _n] ^a O...O = 2.77 ^b O...N = 2.62	Unpublished	[11]
	5-chloro-2-hydroxybenzaldehyde oxime	Dimer [(LH) ₂] ^a O...O = 2.83 ^b O...N = 2.65 ^c R _H = 2.08(1)	CLSALX	[18]
	1-(2-hydroxy-5-ethylphenyl) ethanone oxime	Positional paras not provided	HEPKET	[16]
		Polymer [(LH) _n] ^a O...O = 2.73, 2.75 ^b O...N = 2.51	HEPKET01	[17]
	1-(2-hydroxy-5-methylphenyl) propan-1-one oxime	Positional paras not provided	HMPEKX	[16]
	1-(2-hydroxyphenyl) propan-1-one oxime	Polymer [(LH) _n] ^a O...O = 2.80, 2.79 ^b O...N = 2.53	HELBOP	[23]
	1-(2-hydroxy-5-methylphenyl) ethanone oxime	Positional paras not provided	HMPKET	[16]
	2-hydroxy-5-methoxybenzaldehyde oxime	Polymer [(LH) _n] ^a O...O = 2.82 ^b O...N = 2.65	MXSALO	[19]
	1-(2-hydroxy-5-nonylphenyl) ethanone oxime	Positional paras not provided	HNPKET	[16]
	1-(2-hydroxy-5-methylphenyl) decan-1-one oxime	Positional paras not provided	HMPNKX	[16]
	2-hydroxybenzaldehyde oxime tmeda adduct	^a N...O = 2.64 ^c N...O = 2.67	Unpublished	[13]
	2-hydroxybenzaldehyde oxime diaza-[18]-crown 6 adduct	^b N...O = 2.61 ^d N...O = 2.68	GOBZEC	[22]

^aO...O; separation (Å) of oximic and phenolic oxygen atoms forming inter-molecular hydrogen bonds.^bN...O; separation (Å) of oximic nitrogen and phenolic oxygen atoms forming the intra-molecular hydrogen bonds.^cOxime OH to amine N hydrogen bond. ^dOxime OH to macrocycle N hydrogen bond.^eN₂O₂ donor set hole size (Å) defined as the mean distance of donor atoms from the centroid⁴⁵.

Table 8
List of known phenolic oxime complexes

Complex	CCDC code	Figure	Ref.
<i>Vanadium</i>			
[VO(HsalMe) ₂]	VOSALM	Fig. 16	[12]
[VO(HsalEt)(salEt)] ₂	VOETDI	Fig. 17	[12]
[VO(HsalMe)(salMe)] ₂	VOMEDI	Fig. 18	[12]
[VO{C ₆ H ₄ (O)CH=N–OC(Me)=NH}]	HAXPEB	Fig. 19	[12]
[V ₃ O ₃ (OEt) ₃ (salH) ₂]	POGZIU	Fig. 20	[28]
[VO(OMe)(OC ₆ H ₄ CH=NCHC ₆ H ₄ OC(O)(Me)CHCOMe)]	POGZOA	Fig. 21	[28]
[V ₃ (μ ₃ -O)(HsalH)(salH)(Salmp)][Et ₃ NH] · 2H ₂ O	SUQMOG	Fig. 22	[29]
[VO(HsalH)(salH)] ₂	Unpublished		[11]
<i>Chromium</i>			
[Cr ₆ (μ ₃ -O) ₂ (salH) ₆ (μ ₂ -OOC ₂ H ₅) ₂ (H ₂ O) ₂ (C ₂ H ₅ CN) ₂]	JOYLUE	Fig. 23	[30]
<i>Manganese</i>			
[Mn{(HsalMe)(salMe)} ₄]	Unpublished		[12]
<i>Iron</i>			
[Fe{(salH)(HsalH)} ₄]	BOCCOL	Fig. 24	[2]
[(Me ₃ tacn)Fe(salH) ₃ Fe]	ABOXOE	Fig. 25	[31]
[(Me ₃ tacn) ₂ Fe ₄ (salH) ₂ (μ ₃ -O)(μ ₂ -CH ₃ CO ₂) ₃][PF ₆]	YAYPOD	Fig. 26	[31]
[Fe ₃ O(salmp)(HsalH)(salH)] [–]	TIWKEP	Fig. 27	[32]
<i>Cobalt</i>			
[Co(NO)(HsalMe) ₂]	CEFTEM	Fig. 28	[33]
[Co(salH)(trien)]Cl	ZIFHIF	Fig. 29	[35]
[Co(NO)(HsalH) ₂]	FUPVER		[34]
[Co(NO)(5-Cl–HsalH) ₂]	FUPVIV		[34]
<i>Nickel</i>			
[Ni(HsalH) ₂ (Me ₄ en)]	Unpublished	Fig. 30	[13]
[Ni(HsalH) ₂]	NISALO		[36]
[Ni(HsalMe) ₂]	RIQBAU		[37]
[Ni(HsalEt) ₂]	YOKWOK		[38]
[Ni(5-Me–HsalH) ₂]	HIDQEQ		[39]
[Ni(HsalH) ₂ (N,N'–Me ₂ en)]	Unpublished		[13]
[Ni(HsalH) ₂ (pn)]	Unpublished		[13]
<i>Copper</i>			
[Cu(5-Me–HsalPh) ₂]	Unpublished	Fig. 31	[10]
[Cu(3-CH(OMe) ₂ -5-Me–HsalH) ₂]	RIBYEG	Fig. 32	[44]
[Cu(HsalH) ₂]	SALCOP	Fig. 33	[40]
[Cu(5-Cl–HsalH) ₂]	CSALCU	Fig. 34	[41]
[Cu(HsalMe) ₂]	DEDGAU10	Fig. 35	[42]
[Cu(HsalEt) ₂]	PARHUL		[43]
[Cu(5-Me–HsalH) ₂]	Unpublished		[10]
[Cu(3- <i>i</i> -Bu-5-MeHsalH) ₂]	Unpublished		[10]
[Cu(5-Me–HsalMe) ₂]	HMPMCU		[16]
[Cu(5-Et–HsalMe) ₂]			[16]
[Cu(5-Me–HsalEt) ₂]			[16]
<i>Zinc</i>			
Zn(HsalH) ₂ H ₂ O	TERQEM	Fig. 36	[46]
[Zn(HsalH) ₂] ₂	Unpublished		[11]
<i>Mixed metals</i>			
[(Me ₃ tacn) ₂ Cr ₂ (OMe) ₂ (μ ₃ -O) ₂ (salH) ₂ Mn ₂] ²⁺	HENROH	Fig. 37	[48]
[(Me ₃ tacn) ₂ Cr ₂ (OMe) ₂ (μ ₃ -O) ₂ (salH) ₂ Fe ₂] ²⁺	WAGJIX		[47]
<i>Molybdenum</i>			
[Mo ₂ O ₅ (salH) ₂] ^{2–}	JICHIM	Fig. 38	[49]
<i>Palladium</i>			
[Pd(HsalEt) ₂]	ZIJYIA	Fig. 39	[52]
[Pd(HsalH) ₂]	SAOXPD		[51]
<i>Platinum</i>			
[Pt(HsalH)(Cl)(Me ₂ SO)]	FEQPIA	Fig. 40(a)	[53]
[Pt(3,5-diCl–HsalH)(Cl) ₃ (Me ₂ SO)]	FEQPOG	Fig. 40(b)	[53]

Table 8 (Continued)

Complex	CCDC code	Figure	Ref.
<i>Boron</i>			
[(salH)BPh] ₂	BUCCOR	Fig. 41	[54]
[(HsalH)BPh] ₂	CORGOF	Fig. 42	[55]
<i>Gallium</i>			
[GaMe(HsalH) ₂]	VUBRUF	Fig. 43	[56]
<i>Tin</i>			
[(Bu ₂ Sn)(Bu ₂ SnO)(Bu ₂ SnOH)(HsalH)(salH)]	WEVGIN	Fig. 44	[57]
[(Me ₂ Sn)(Me ₂ SnO)(Me ₂ SnON=CHPh)(HsalH)(salH)]	NOMYAP	Fig. 45	[59]
[(Me ₂ Sn)(Me ₂ SnO)(Me ₂ SnO–C ₆ H ₄ - <i>p</i> -Me)(HsalH)(salH)]	NOMYET		[59]
[(Me ₂ Sn)(Me ₂ SnO)(Me ₂ SnO–C ₆ H ₄ - <i>p</i> -Br)(HsalH)(salH)]	NOMYIX		[59]
[(Me ₂ Sn)(Me ₂ SnO)(Me ₂ SnO–Me)(HsalH)(salH)]	ZUYRUG		[58]
[(Me ₂ Sn)(Me ₂ SnO)(Me ₂ SnO–Et)(HsalH)(salH)]	ZUYSAN		[58]
[(Me ₂ Sn)(Me ₂ SnO)(Me ₂ SnO– ^{<i>n</i>} Pr)(HsalH)(salH)]	ZUYSER		[58]
[(Me ₂ Sn)(Me ₂ SnO)(Me ₂ SnO– ^{<i>i</i>} Pr)(HsalH)(salH)]	ZUTSIV		[58]
[(Me ₂ Sn)(Me ₂ SnO)(Me ₂ SnO–CH ₂ CH(Me)CH ₂ CH ₃)(HsalH)(salH)]	SOZQAZ		[60]
[(Me ₂ Sn)(Me ₂ SnO)(Me ₂ SnO–NCHC ₆ H ₄ - <i>o</i> -OH)(HsalH)(salH)]	BAXXAZ		[61]
[(Me ₂ Sn)(Me ₂ SnO)(Me ₂ SnF)(HsalH)(salH)]	BAXXED		[61]

to explaining the high ‘strength’ and selectivity of these reagents when used in the solvent extraction of copper(II). It is also consistent with the observation that in commercial operations many of the ‘modifiers’ added to formulations to ‘weaken’ the extractant are themselves likely to form strong hydrogen bonds to the uncomplexed ligand. The survey identifies metal types and oxidation levels which are likely to lead to formation of insoluble (polynuclear) metal complexes. Such information should be useful to those developing flowsheets to treat new types of pregnant leach solutions containing mixtures of transition metal ions.

Acknowledgements

We are grateful to Avecia’s Metal Extraction Products Business for funding to support Dr. Andrew G. Smith and Dr. David J. White, to Professor C.D. Garner and Professor M. McPartlin and Dr. J. Griggs, Dr. L. Drummond, Dr. V. Hultgen (nee Jones) and Dr. A. Zissimos for permission to refer to structures in Ph.D. theses (see references), and to Dr. A. Parkin for assistance in generating Fig. 25.

References

- [1] G.A. Kordosky, in: K.C. Sole, P.M. Cole, J.S. Preston, D.A. Robinson (Eds.), Proceedings of the International Solvent Extraction Conference, South African Institute of Mining and Metallurgy, Johannesburg, 2002, pp. 853–862.
- [2] J.M. Thorpe, R.L. Beddoes, D. Collison, C.D. Garner, M. Helliwell, J.M. Holmes, P.A. Tasker, *Angew. Chem. Int. Ed.* 38 (1999) 1119.
- [3] J. Szymanowski, *Hydroxyoximes and Copper Hydrometallurgy*, CRC Press, London, 1993.
- [4] W.G. Davenport, in: G.A. Eltringham, N.L. Piret, M. Sahoo (Eds.), Proceedings of Copper99–Cobre99 International Conference, The Minerals, Metals and Materials Society, 1999.
- [5] J. Szymanowski, *Hydroxyoximes and Copper Hydrometallurgy*, CRC Press, London, 1993, pp. 117–140.
- [6] M.P. Elizalde, J.M. Castresana, M. Aguilar, M. Cox, *Chem. Scr.* 25 (1985) 300.
- [7] P. Chaudhuri, M. Winter, P. Fleischhauer, W. Haase, U. Flörke, H.-J. Haupt, *Inorg. Chim. Acta* 212 (1993) 241.
- [8] E. Bill, C. Krebs, M. Winter, M. Gerdan, A.X. Trautwein, U. Flörke, H.-J. Haupt, P. Chaudhuri, *Chem. Eur. J.* 3 (1997) 193.
- [9] F.H. Allen, O. Kennard, *Chem. Des. Automation News* 8 (1993) 31.
- [10] L.A. Drummond, Ph.D. thesis, Polytechnic of North London, 1989.
- [11] J.M. Thorpe, Ph.D. thesis, University of Manchester, 1992.
- [12] J. Grigg, Ph.D. thesis, University of Manchester, 1994.
- [13] V. Jones, Ph.D. thesis, University of Manchester, 1997.
- [14] L.L. Merritt, Jr., E. Schroeder, *Acta Crystallogr.* 9 (1956) 194.
- [15] C.E. Pfluger, R.L. Harlow, *Acta Crystallogr. Sect. B* 29 (1973) 2608.
- [16] A. Koziol, Z. Kosturkiewicz, *Pol. J. Chem.* 53 (1979) 1393.
- [17] A. Koziol, Z. Kosturkiewicz, *Pol. J. Chem.* 58 (1984) 569.
- [18] S.H. Simonsen, C.E. Pfluger, C.M. Thompson, *Acta Crystallogr.* 14 (1961) 269.
- [19] C.E. Pfluger, M.T. Pfluger, E.B. Brackett, *Acta Crystallogr. Sect. B* 34 (1978) 1017.
- [20] J.W. Hosking, N.M. Rice, *Hydrometallurgy* 3 (1978) 217.
- [21] I. Komasa, T. Otake, A. Yamada, *J. Chem. Eng. Jpn.* 13 (1980) 130.
- [22] W.H. Watson, F. Vögtle, W.M. Müller, *J. Inclusion Phenom.* 6 (1988) 491.
- [23] J.K. Maurin, *Acta Crystallogr. Sect. C* 50 (1994) 1357.
- [24] H.J. Bielig, H. Möllinger, *Liebigs. Ann. Chem.* 605 (1957) 117.
- [25] R. Lundqvist, A. Panfilov, N. Kalinchenko, I. Marov, *Acta Chem. Scand. A30* (1976) 515.
- [26] I. Rani, K.B. Pandeya, R.P. Singh, *Indian J. Chem.* 21A (1982) 502.
- [27] J. Grigg, D. Collison, C.D. Garner, M. Helliwell, P.A. Tasker, J.M. Thorpe, *J. Chem. Soc. Chem. Commun.* (1993) 1807.
- [28] V. Zerbib, F. Robert, P. Gouzerh, *J. Chem. Soc. Chem. Commun.* (1994) 2179.

- [29] P. Chaudhuri, M. Hess, T. Weyhermüller, E. Bill, H.-J. Haupt, U. Flörke, *Inorg. Chem. Commun.* 1 (1998) 39.
- [30] P. Chaudhuri, M. Hess, E. Reutschler, T. Weyhermüller, U. Flörke, *New. J. Chem.* (1998) 553.
- [31] (a) P. Chaudhuri, M. Winter, P. Fleischhauer, W. Haase, U. Flörke, H.-J. Haupt, *Inorg. Chim. Acta* 212 (1993) 241;
(b) P. Chaudhuri, *Proc. Indian Acad. Sci. (Chem. Sci.)* 111 (1999) 397.
- [32] E. Bill, C. Krebs, M. Winter, M. Gerdan, A.X. Trautwein, U. Flörke, H.-J. Haupt, P. Chaudhuri, *Chem. Eur. J.* 3 (1997) 193.
- [33] L.F. Larkworthy, D.C. Povey, *J. Crystallogr. Spectrosc. Res.* 13 (1983) 413.
- [34] M. Gallagher, M.F.C. Ladd, L.F. Larkworthy, D.C. Povey, K.A.R. Salib, *J. Crystallogr. Spectrosc. Res.* 16 (1986) 967.
- [35] E. Toyota, K. Umakoshi, Y. Yamamoto, *Bull. Chem. Soc. Jpn.* 68 (1995) 858.
- [36] R.C. Srivastava, E.C. Lingafelter, P.C. Jain, *Acta Crystallogr.* 22 (1967) 922.
- [37] A.G. Hatzidimitriou, M. Uddin, M. Lalia-Kantouri, *Z. Anorg. Allg. Chem.* 623 (1997) 627.
- [38] M. Lalia-Kantouri, M. Hartophylles, P.D. Jannakoudakis, G.P. Voutsas, *Z. Anorg. Allg. Chem.* 621 (1995) 645.
- [39] G.P. Voutsas, K.G. Keramidas, E. Dova, M. Lalia-Kantouri, M. Hartophylles, *Z. Kristallogr.—New Cryst. Struct.* 33 (1999) 214.
- [40] M.A. Jarski, E.C. Lingafelter, *Acta Crystallogr.* 17 (1964) 1109.
- [41] P.L. Orioli, E.C. Lingafelter, B.W. Brown, *Acta Crystallogr.* 17 (1964) 1113.
- [42] (a) Z. Kangjing, Z. Chengming, C. Xing, Y. Chenge, *Kexue Tongbao (Chin.)* 30 (1985) 266;
(b) Z. Kangjing, Z. Chengming, C. Xing, Y. Chenge, *Kexue Tongbao (Chin.)* 30 (1985) 1484.
- [43] M. Lalia-Kantouri, M. Uddin, C.C. Hadjikostas, H. Papanikolas, G. Palios, S. Anagnostis, V. Anesti, *Z. Anorg. Allg. Chem.* 623 (1997) 1983.
- [44] E.V. Rybak-Akimova, D.H. Busch, P.K. Kahol, N. Pinto, N.W. Alcock, H.J. Clase, *Inorg. Chem.* 36 (1997) 510.
- [45] K. Henrick, P.A. Tasker, L.F. Lindoy, *Prog. Inorg. Chem.* 33 (1985) 1.
- [46] I. Potocnak, F.W. Heinemann, M. Rausch, D. Steinborn, *Acta Crystallogr. Sect. C* 53 (1997) 54.
- [47] P. Chaudhuri, M. Winter, P. Fleischhauer, W. Haase, U. Flörke, H.-J. Haupt, *J. Chem. Soc. Chem. Commun.* (1993) 566.
- [48] P. Chaudhuri, F. Birkelbach, M. Winter, V. Staemmlar, P. Fleischhauer, W. Haase, U. Flörke, H.-J. Haupt, *J. Chem. Soc. Dalton Trans.* (1994) 2313.
- [49] S. Liu, H. Zhu, J. Zubieta, *Polyhedron* 8 (1989) 2473.
- [50] S.H. Simonsen, C.E. Pfluger, *Acta Crystallogr.* 10 (1957) 536.
- [51] C.E. Pfluger, R.L. Harlow, S.H. Simonsen, *Acta Crystallogr. Sect. B* 26 (1970) 1631.
- [52] G.P. Voutsas, K.G. Keramidas, M. Lalia-Kontouri, *Polyhedron* 15 (1996) 147.
- [53] Y.N. Kukushkin, V.K. Krylov, S.F. Kaplan, M. Calligaris, E. Zangrando, A.J.L. Pombeiro, V.Y. Kukushkin, *Inorg. Chim. Acta* 285 (1999) 116.
- [54] S.J. Rettig, J. Trotter, *Can. J. Chem.* 13 (1983) 206.
- [55] W. Kliegel, S.J. Rettig, J. Trotter, *Can. J. Chem.* 62 (1984) 1363.
- [56] S.J. Rettig, A. Storr, J. Trotter, *Acta Crystallogr. Sect. C* 48 (1992) 1587.
- [57] F. Kayser, M. Biesemans, M. Bouâlam, E.R.T. Tiekink, A. El Khoulfi, J. Meunier-Piret, A. Bouhdid, K. Jurkschat, M. Gielen, R. Willem, *Organometallics* 13 (1994) 1098.
- [58] R. Willem, A. Bouhdid, F. Kayser, A. Delmotte, M. Gielen, J.C. Martins, M. Biesemans, B. Mahieu, E.R.T. Tiekink, *Organometallics* 15 (1996) 1920.
- [59] R. Willem, A. Bouhdid, A. Meddour, C. Camacho-Camacho, F. Mercier, M. Gielen, M. Biesemans, F. Ribot, C. Sanchez, E.R.T. Tiekink, *Organometallics* 16 (1997) 4377.
- [60] A. Meddour, A. Bouhdid, M. Gielen, M. Biesemans, F. Mercier, E.R.T. Tiekink, R. Willem, *Eur. J. Inorg. Chem.* (1998) 1467.
- [61] F.A.G. Mercier, A. Meddour, M. Gielen, M. Biesemans, R. Willem, E.R.T. Tiekink, *Organometallics* 17 (1998) 5933.
- [62] A. Meddour, F. Mercier, J.C. Martins, M. Gielen, M. Biesemans, R. Willem, *Inorg. Chem.* 36 (1997) 5712.
- [63] J.C. Martins, M. Biesemans, R. Willem, *Prog. NMR Spectrosc.* 36 (2000) 271.